Parametrized Partial Differential Equations

Heat Transfer
Back-of-the-Envelope Calculations: Model Simplification, Model Order Reduction

Anthony T Patera, MIT

Mathematics of Reduced Order Models
ICERM
Providence, RI, USA

February 19, 2020

pPDEs

Heat Transfer
Back-of-the-Envelope Calculations: Model Simplification, Model Order Reduction

Anthony T Patera, MIT

Mathematics of Reduced Order Models
ICERM
Providence, RI, USA

February 19, 2020

Acknowledgments

Collaborators:

- J Penn — MIT
- K Kaneko, P Fischer, P-H Tsai — U Illinois
- T Taddei — INRIA Bordeaux
- P Huynh, D Knezevic, L Nguyen — Akselos SA
- Students in 2.51 Intermediate Heat and Mass Transfer — MIT

Financial Support: AFOSR, ONR, ARO

Perspective

Back-of-the-Envelope Calculation (Figurative)

Definition (Wikipedia)

A *back-of-the-envelope* calculation is a rough calculation, typically jotted down on any available scrap of paper such as an envelope. It is more than a guess but less than an accurate calculation or mathematical proof.

The defining characteristic of back-of-the-envelope calculations is the use of simplified assumptions.

Single-Screen Script (Literal)

Definition (Paterapedia)

A *single-screen script* is a rough prediction, implemented with a *limited instruction set* in a code which can be viewed in its entirety on a single screen. It is more than a guess but less than an accurate calculation or mathematical proof.

A defining characteristic of single-screen script predictions is the use of model simplification.

Relevance to Workshop

Definition (Paterapedia)

A *single-screen script* is a rough prediction, implemented with a *limited instruction set* in a code which can be viewed in its entirety on a single screen. It is more than a guess but less than an accurate calculation or mathematical proof.

A defining characteristic of single-screen script predictions is the use of model simplification.

The limited instruction set is (for heat transfer)...

Relevance to Workshop

Definition (Paterapedia)

A *single-screen script* is a rough prediction, implemented with a *limited instruction set* in a code which can be viewed in its entirety on a single screen. It is more than a guess but less than an accurate calculation or mathematical proof.

A defining characteristic of single-screen script predictions is the use of model simplification.

The limited instruction set is (for heat transfer). . . a set of pPDEs.

Questions to Ponder: 2020

Why do we teach students Back-of-the-Envelope — succinct, transparent, fast — methods of engineering analysis still in 2020?

Questions to Ponder: 2020

Why do we teach students Back-of-the-Envelope — succinct, transparent, fast — methods of engineering analysis still in 2020?

Why do engineers practice Back-of-the-Envelope calculations — in tandem with large-scale simulation — still in 2020?

Questions to Ponder: 2020

Why do we teach students Back-of-the-Envelope — succinct, transparent, fast — methods of engineering analysis still in 2020?

Why do engineers practice Back-of-the-Envelope calculations — in tandem with large-scale simulation — still in 2020?

How can we study Back-of-the-Envelope engineering analysis through the lens of undergraduate education (2.51)?

Questions to Ponder: 2020

Why do we teach students Back-of-the-Envelope — succinct, transparent, fast — methods of engineering analysis still in 2020?

Why do engineers practice Back-of-the-Envelope calculations — in tandem with large-scale simulation — still in 2020?

How can we study Back-of-the-Envelope engineering analysis through the lens of undergraduate education (2.51)?

How can the Back-of-the-Envelope benefit — without losing essential advantages — from computational advances 1960-2020?

Questions to Ponder: 2020

Why do we teach students Back-of-the-Envelope — succinct, transparent, fast — methods of engineering analysis still in 2020?

Why do engineers practice Back-of-the-Envelope calculations — in tandem with large-scale simulation — still in 2020?

How can we study Back-of-the-Envelope engineering analysis through the lens of undergraduate education (2.51)?

How can the Back-of-the-Envelope benefit — without losing essential advantages — from pMOR advances 1960-2020?

Questions to Ponder: 2020

Why do we teach students Back-of-the-Envelope — succinct, transparent, fast — methods of engineering analysis still in 2020?

Why do engineers practice Back-of-the-Envelope calculations — in tandem with large-scale simulation — still in 2020?

How can we study Back-of-the-Envelope engineering analysis through the lens of undergraduate education (2.51)?

How can the Back-of-the-Envelope benefit — without losing essential advantages — from pMOR advances 1960-2020?

Is the Back-of-the Envelope fundamentally a human activity, or can it be viewed more formally as an algorithm or framework?

Future Prospects: 2030

Headline:

Artificial Student Earns A+ in MIT Subject 2.51

Implications: in engineering education

How should we change *what* we teach,
and *how* we teach?

How should we change our assessment of (human) students?

and downstream, in professional engineering practice,

How can we enhance prediction procedures?

General theme: integrated methodology
for mathematical modeling and computation.

First (very brittle) steps: Artie [44].

Macroscale Heat Transfer. . .

S Austin 2.51

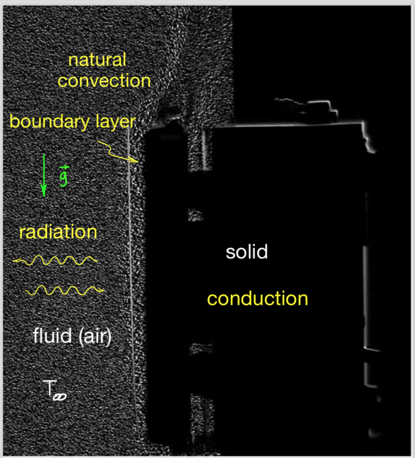

External Flows

Conduction, Forced and Natural Convection (Gravity-Induced), Radiation

. . . in Everyday Life (and Beyond)

2.51 Project Case Studies

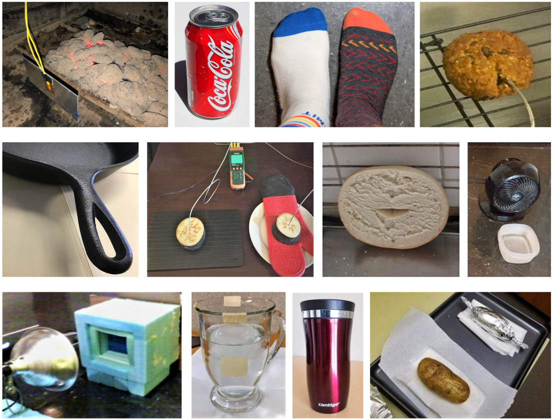

Key Topics

Review of Heat Transfer

Heat Transfer (2.51) Back-of-the-Envelope Framework

Examples from 2.51 Project Case Studies

Opportunities for Parametrized Model Order Reduction

Thread: Parametrized Partial Differential Equations

Heat Transfer 101

via the *Dunk* Problem

Macroscale Heat Transfer. . . S Austin 2.51

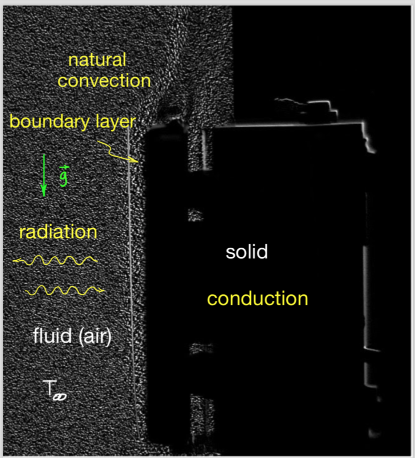

External Flows

Conduction, Forced and Natural Convection (Gravity-Induced), Radiation

Motivation and Notation

P Phan 2.51

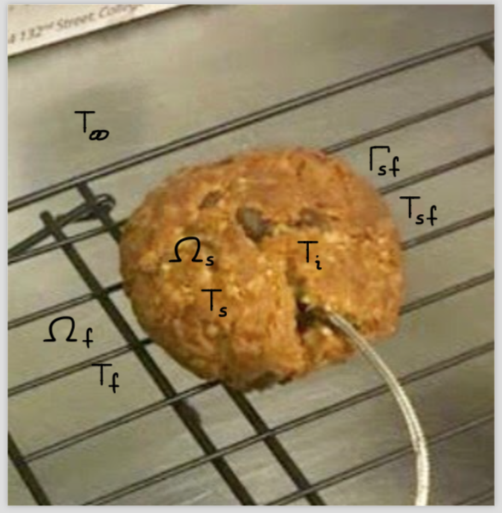

An Idealized Configuration

Let $\Omega \subset \mathbb{R}^3$, $\overline{\Omega} = \overline{\Omega_\text{s}} \cup \overline{\Omega_\text{f}}$:

$\Omega_\text{f} \equiv$ fluid (air) domain: effectively infinite;

$\Omega_\text{s} \equiv$ solid domain: convex, (single, scale) parameter ℓ;

$\Gamma_\text{sf} \equiv \overline{\Omega_\text{s}} \cap \overline{\Omega_\text{f}} \setminus \overline{\Gamma_\text{s}^\text{ad}}$; $\qquad \partial\Omega_\text{s} \equiv \overline{\Gamma_\text{sf}} \cup \overline{\Gamma_\text{s}^\text{ad}}$

uniformly large enclosure: $\text{dist}(\Omega_\text{s}, \partial\Omega) \gg \ell$;

coordinate system: $x \equiv (x_1, x_2, x_3)$, $\{\mathbf{e}_i\}_i$; gravity $\mathbf{g} = -g\mathbf{e_2}$.

Initial conditions: $T|_{\Omega_\text{s}} \equiv T_\text{s} = T_\text{i}$ uniform, $T|_{\Omega_\text{f}} \equiv T_\text{f} = T_\infty$;
assume $T_\text{i} > T_\infty$ (wlog).

Farfield conditions: *quiescent* fluid; $T_\text{f} = T_\infty$ (on $\partial\Omega$) — implicit.

Governing Equations: Dimensional

Find $[V \equiv (V_1, V_2, V_3), T](x, t)$ $\qquad T_\mathrm{s} = T|_{\Omega_\mathrm{s}}, T_\mathrm{f} = T|_{\Omega_\mathrm{f}}$

$$\frac{\partial V}{\partial t} + V \cdot \nabla V = -\nabla \frac{p}{\rho_\infty} + g\beta(T_\mathrm{f} - T_\infty)\mathbf{e}_2 + \nu \nabla^2 V \text{ in } \Omega_\mathrm{f}, t > 0\,,$$

$$\nabla \cdot V = 0 \text{ in } \Omega_\mathrm{f}, t > 0\,,$$

$$\frac{\partial T_\mathrm{f}}{\partial t} + V \cdot \nabla T_\mathrm{f} = \alpha_\mathrm{f} \nabla^2 T_\mathrm{f} \text{ in } \Omega_\mathrm{f}, t > 0\,,$$

$$\frac{\partial T_\mathrm{s}}{\partial t} = \alpha_\mathrm{s} \nabla^2 T_\mathrm{s} \text{ in } \Omega_\mathrm{s}, t > 0\,,$$

$$T_\mathrm{s} = T_\mathrm{f},\ -k_\mathrm{s} \nabla T_\mathrm{s} \cdot \hat{\mathbf{n}} = -k \nabla T_\mathrm{f} \cdot \hat{\mathbf{n}} + \varepsilon_\mathrm{r} \sigma_\mathrm{SB} (T_\mathrm{s}^4 - T_\infty^4) \text{ on } \Gamma_\mathrm{sf}, t > 0\,,$$

$$T_\mathrm{s}(\cdot, t = 0) = T_\mathrm{i} \text{ in } \Omega_\mathrm{s},\ T_\mathrm{f}(\cdot, t = 0) = T_\infty \text{ in } \Omega_\mathrm{f}\,.$$

Fluid Domain and Wall

S Austin 2.51

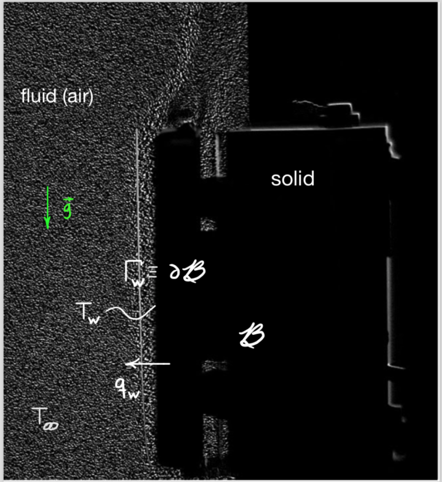

$\mathrm{HTC_c}$: Definition

Consider solid body $\mathcal{B}$ surrounded by fluid; define wall $\Gamma_\mathrm{w} \equiv \partial\mathcal{B}$.

Given: wall Γ_w approximately *iso*thermal at temperature T_w;

fluid far from wall at temperature T_∞ (and quiescent).

The *spatial-averaged* convection $\mathrm{HTC_c}$ is defined as

$$\langle \bar{\eta}_\mathrm{c}^\mathrm{iso} \rangle [T_\mathrm{w}] \equiv \frac{\langle Q_\mathrm{w} \rangle}{|\Gamma_\mathrm{w}|(T_\mathrm{w} - T_\infty)}$$

for

$Q_\mathrm{w} \equiv \int_{\Gamma_\mathrm{w}} q_\mathrm{w} \, dS \equiv$ heat transfer rate from wall to fluid,

$q_\mathrm{w} \equiv$ heat flux from wall to fluid,

$|\Gamma_\mathrm{w}| \equiv$ the surface area of wall Γ_w;

$\langle \cdot \rangle \equiv$ steady-state or long-time-average operator.

Newton's Law of Cooling

By construction: $\langle Q_\mathrm{w}\rangle \equiv \int_{\Gamma_\mathrm{w}} q_\mathrm{w}\, dS = \langle \bar{\eta}_\mathrm{c}^\mathrm{iso}\rangle [T_\mathrm{w}] \cdot |\Gamma_\mathrm{w}| (T_\mathrm{w} - T_\infty)$.

Heat flux q_w:

$$\begin{aligned} q_\mathrm{w} &\equiv -k_\mathrm{f} \nabla T_\mathrm{f} \cdot \hat{\mathbf{n}} \quad \text{Fourier's Law (in fluid)} \\ &\approx -k_\mathrm{f} \frac{(T_\infty - T_\mathrm{w})}{\delta^\mathrm{bl}(x_\mathrm{s})} \quad \delta^\mathrm{bl}\text{: thermal boundary layer;} \end{aligned}$$

but for laminar natural convection, δ^bl depends weakly on x_s,

$$\delta^\mathrm{bl}(x_\mathrm{s}) \sim \alpha_\mathrm{f}^{1/2} (g\beta |T_\mathrm{w} - T_\infty|)^{-1/4}\, x^{1/4}$$

hence

$$q_\mathrm{w} \approx \langle \bar{\eta}_\mathrm{c}^\mathrm{iso}\rangle [T_\mathrm{w}] \cdot (T_\mathrm{w} - T_\infty) \text{ on } \Gamma_\mathrm{w} \textit{ uniform.}$$

Boundary Layer Visualization

S Austin 2.51

Background-Oriented Schlieren

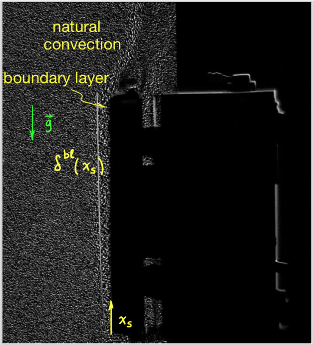

$$\delta^{\mathrm{bl}}(x_{\mathrm{s}}) \sim \sqrt{\alpha_{\mathrm{f}} t^{\text{L-E}}(x_{\mathrm{s}})} = \sqrt{\alpha_{\mathrm{f}} x_{\mathrm{s}} / \mathcal{U}_{\mathrm{buoy}}(x_{\mathrm{s}})}$$

$$\mathcal{U}_{\mathrm{buoy}}(x_{\mathrm{s}}) \sim \sqrt{g \beta |T_{\mathrm{w}} - T_{\infty}| x_{\mathrm{s}}}$$

Solid and Fluid Domains

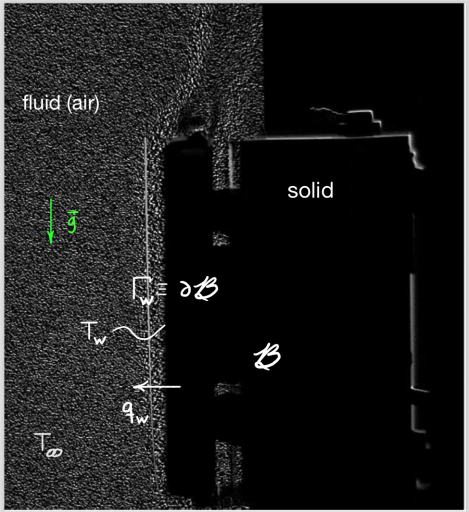

Dirichlet-Neumann Map ⇒ Robin Condition

Now assume T_w is not known, but part of solution for T_s in $\mathcal{B}$.

Boundary condition on solid body $\mathcal{B}$:

$$\begin{aligned} -k_\mathrm{s} \nabla T_\mathrm{s} \cdot \hat{\mathbf{n}} &= -k_\mathrm{f} \nabla T_\mathrm{f} \cdot \hat{\mathbf{n}} \quad \text{(First Law)} \\ &= q_\mathrm{w} \\ &\approx \langle \bar{\eta}_\mathrm{c}^\mathrm{iso} \rangle [T_\mathrm{w}] \cdot (T_\mathrm{w} - T_\infty). \end{aligned}$$

Dirichlet-Neumann Map ⇒ Robin Condition

Now assume T_w is not known, but part of solution for T_s in $\mathcal{B}$.

Boundary condition on solid body $\mathcal{B}$:

$$\begin{aligned} -k_\mathrm{s}\nabla T_\mathrm{s}\cdot\hat{\mathbf{n}} &= -k_\mathrm{f}\nabla T_\mathrm{f}\cdot\hat{\mathbf{n}} \quad \text{(First Law)} \\ &= q_\mathrm{w} \\ &\approx \langle\bar{\eta}_\mathrm{c}^\mathrm{iso}\rangle[T_\mathrm{f}]\cdot(T_\mathrm{f} - T_\infty) \end{aligned}$$

Dirichlet-Neumann Map $\Rightarrow$ Robin Condition

Now assume T_{w} is not known, but part of solution for T_{s} in $\mathcal{B}$.

Boundary condition on solid body $\mathcal{B}$:

$$
\begin{aligned}
-k_{\mathrm{s}} \nabla T_{\mathrm{s}} \cdot \hat{\mathbf{n}} &= -k_{\mathrm{f}} \nabla T_{\mathrm{f}} \cdot \hat{\mathbf{n}} \quad \text{(First Law)} \\
&= q_{\mathrm{w}} \\
&\approx \langle \bar{\eta}_{\mathrm{c}}^{\mathrm{iso}} \rangle [T_{\mathrm{s}}] \cdot (T_{\mathrm{s}} - T_{\infty})
\end{aligned}
$$

Dirichlet-Neumann Map $\Rightarrow$ Robin Condition

Now assume T_{w} is not known, but part of solution for T_{s} in $\mathcal{B}$.

Boundary condition on solid body $\mathcal{B}$:

$$\begin{aligned} -k_{\mathrm{s}} \nabla T_{\mathrm{s}} \cdot \hat{\mathbf{n}} &= -k_{\mathrm{f}} \nabla T_{\mathrm{f}} \cdot \hat{\mathbf{n}} \quad \text{(First Law)} \\ &= q_{\mathrm{w}} \\ &\approx \langle \bar{\eta}_{\mathrm{c}}^{\mathrm{iso}} \rangle [T_{\mathrm{s}}] \cdot (T_{\mathrm{s}} - T_{\infty}) \end{aligned}$$

if isothermal wall condition is approximately satisfied.

Condition for approximately isothermal wall: *either*

$$\mathrm{Bi}_{\mathrm{c}}[T_{\mathrm{w}}] \text{ (Biot Number) } \equiv \frac{\langle \bar{\eta}_{\mathrm{c}}^{\mathrm{iso}} \rangle [T_{\mathrm{w}}]\, \mathcal{L}}{k_{\mathrm{s}}} \ll 1 \ ,$$

for $\mathcal{L}$ an appropriate length scale in solid body.

Argument: $\frac{k_{\mathrm{s}} (\Delta T)_{\mathrm{in}\ \mathcal{B}}}{\mathcal{L}} \approx \langle \bar{\eta}_{\mathrm{c}}^{\mathrm{iso}} \rangle [T_{\mathrm{w}}] \cdot (T_{\mathrm{w}} - T_{\infty}) \Rightarrow \frac{(\Delta T)_{\mathrm{in}\ \mathcal{B}}}{|T_{\mathrm{w}} - T_{\infty}|} \ll 1$.

Dirichlet-Neumann Map ⇒ Robin Condition

Now assume T_{w} is not known, but part of solution for T_{s} in $\mathcal{B}$.

Boundary condition on solid body $\mathcal{B}$:

$$\begin{aligned} -k_{\mathrm{s}} \nabla T_{\mathrm{s}} \cdot \hat{\mathbf{n}} &= -k_{\mathrm{f}} \nabla T_{\mathrm{f}} \cdot \hat{\mathbf{n}} \quad \text{(First Law)} \\ &= q_{\mathrm{w}} \\ &\approx \langle \bar{\eta}_{\mathrm{c}}^{\mathrm{iso}} \rangle [T_{\mathrm{s}}] \cdot (T_{\mathrm{s}} - T_{\infty}) \end{aligned}$$

if isothermal wall condition is approximately satisfied.

Condition for approximately isothermal wall: *or*

$$\mathrm{Bi}_{\mathrm{c}}[T_{\mathrm{w}}] \text{ (Biot Number) } \equiv \frac{\langle \bar{\eta}_{\mathrm{c}}^{\mathrm{iso}} \rangle [T_{\mathrm{w}}]\, \mathcal{L}}{k_{\mathrm{s}}} \gg 1 \ ,$$

for $\mathcal{L}$ an appropriate length scale in solid body.

Argument: $\frac{k_s (\Delta T)_{\text{in } \mathcal{B}}}{\mathcal{L}} \approx \langle \bar{\eta}_{\mathrm{c}}^{\mathrm{iso}} \rangle [T_{\mathrm{w}}] \cdot (T_{\mathrm{w}} - T_{\infty}) \Rightarrow \ T_{\mathrm{w}} \to T_{\infty}$.

HTC$_\mathrm{c}$: Measurement [11, 25]

Given heat source Q_source in solid body,

measure wall temperature at several locations, $\{T_\mathrm{w}\}$,

measure farfield fluid temperature, T_∞,

evaluate $\langle \bar{\eta}_\mathrm{c}^\mathrm{iso} \rangle [T_\mathrm{w}^\mathrm{avg}] = \dfrac{Q_\mathrm{source}}{|\Gamma_\mathrm{w}|(T_\mathrm{w}^\mathrm{avg} - T_\infty)}$.

Confirm condition for isothermal wall:

theory: $\mathrm{Bi}_\mathrm{c}[T_\mathrm{w}^\mathrm{avg}]$ (Biot Number) $\equiv \dfrac{\langle \bar{\eta}_\mathrm{c}^\mathrm{iso} \rangle [T_\mathrm{w}^\mathrm{avg}]\,\mathcal{L}}{k_\mathrm{s}} \ll 1$;

experiment: $\mathrm{std\_dev}\{T_\mathrm{w}\} \ll |T_\mathrm{w} - T_\infty|$.

$\mathrm{HTC_c}$ Functions: Experimental Correlations [35, 2]

For given $\mathrm{HTC_c}$ configuration:

Introduce length scale associated with $\Gamma_{\mathrm{w}}, \mathcal{B}$: ℓ.

Form nondimensional groups:

$$\langle \overline{\mathrm{Nu}_\ell} \rangle \equiv \frac{\langle \bar{\eta}_{\mathrm{c}}^{\mathrm{iso}} \rangle [T_{\mathrm{w}}]\, \ell}{k_{\mathrm{f}}} \;;$$

$$\mathrm{Ra}_\ell^{\mathrm{w}} \equiv \frac{g\beta |T_{\mathrm{w}} - T_\infty| \ell^3}{\alpha_{\mathrm{f}} \nu}, \;\; \mathrm{Pr} \equiv \frac{\nu}{\alpha_{\mathrm{f}}}\,.$$

Define parameter: $\mu \equiv (\mathrm{Ra}_\ell^{\mathrm{w}}, \mathrm{Pr}) \in \mathcal{P} \subset \mathbb{R}_+^2$.

Fit to data: $\mathbb{F}_{\mathrm{HTC_c}} : \mu \in \mathcal{P} \mapsto \langle \overline{\mathrm{Nu}_\ell} \rangle \in \mathbb{R}_+$;

$$\langle \bar{\eta}_{\mathrm{c}}^{\mathrm{iso}} \rangle \, [T_{\mathrm{w}}] = \frac{k_{\mathrm{f}}}{\ell} \langle \overline{\mathrm{Nu}_\ell} \rangle.$$

Example: HTC_c Correlation — Vertical Plate [35]

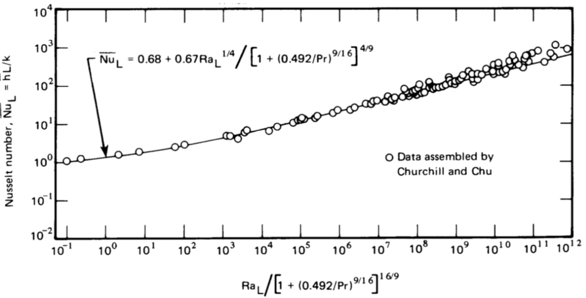

Figure 8.3 The correlation of $\overline{h}$ data for vertical isothermal surfaces by Churchill and Chu [8.3], using $\text{Nu}_L = \text{fn}(\text{Ra}_L, \text{Pr})$. (Applies to full range of Pr.)

Extension: orientation relative to gravity, (θ_g, φ_g).

Example: $\mathrm{HTC_c}$ Correlation — Horizontal Cylinder [35]

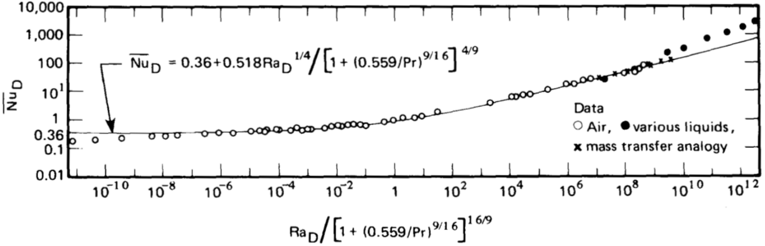

Figure 8.6 The data of many investigators for heat transfer from isothermal horizontal cylinders during natural convection, as correlated by Churchill and Chu [8.8].

Stefan-Boltzmann Law: Graybodies

Wall flux: for convex body in large enclosure

$$q_{\mathrm{w}} = \langle \bar{\eta}_{\mathrm{c}}^{\mathrm{iso}} \rangle [T_{\mathrm{w}}](T_{\mathrm{w}} - T_{\infty}) + \varepsilon_{\mathrm{r}} \sigma_{\mathrm{SB}} (T_{\mathrm{w}}^4 - T_{\infty}^4)$$

Stefan-Boltzmann Law: Graybodies

Wall flux: for convex body in large enclosure

$$q_{\mathrm{w}} = \langle \bar{\eta}_{\mathrm{c}}^{\mathrm{iso}} \rangle [T_{\mathrm{w}}](T_{\mathrm{w}} - T_{\infty}) + \varepsilon_{\mathrm{r}} \sigma_{\mathrm{SB}} (T_{\mathrm{w}}^2 + T_{\infty}^2)(T_{\mathrm{w}}^2 - T_{\infty}^2)$$

Stefan-Boltzmann Law: Graybodies

Wall flux: for convex body in large enclosure

$$q_{\mathrm{w}} = \langle \bar{\eta}_{\mathrm{c}}^{\mathrm{iso}} \rangle [T_{\mathrm{w}}](T_{\mathrm{w}} - T_{\infty}) + \varepsilon_{\mathrm{r}} \sigma_{\mathrm{SB}} (T_{\mathrm{w}}^2 + T_{\infty}^2)(T_{\mathrm{w}} + T_{\infty})(T_{\mathrm{w}} - T_{\infty})\,;$$

Stefan-Boltzmann Law: Graybodies

Wall flux: for convex body in large enclosure

$$q_{\mathrm{w}} = \langle \bar{\eta}_{\mathrm{c}}^{\mathrm{iso}} \rangle [T_{\mathrm{w}}](T_{\mathrm{w}} - T_{\infty}) + \varepsilon_{\mathrm{r}} \sigma_{\mathrm{SB}} (T_{\mathrm{w}}^2 + T_{\infty}^2)(T_{\mathrm{w}} + T_{\infty})(T_{\mathrm{w}} - T_{\infty})\,;$$

$$\tilde{q}_{\mathrm{w}} = \overbrace{(\tilde{\eta}_{\mathrm{c}} + \tilde{\eta}_{\mathrm{r}})}^{\tilde{\eta}}(T_{\mathrm{w}} - T_{\infty})\,.$$

Nonlinear Case: $\tilde{\eta}^{\mathrm{nlin}}(T_{\mathrm{w}})$ "exact"

$$\tilde{\eta}_{\mathrm{c}}^{\mathrm{nlin}} = \langle \bar{\eta}_{\mathrm{c}}^{\mathrm{iso}} \rangle [T_{\mathrm{w}}];\ \tilde{\eta}_{\mathrm{r}}^{\mathrm{nlin}} = \varepsilon_{\mathrm{r}} \sigma_{\mathrm{SB}} (T_{\mathrm{w}}^2 + T_{\infty}^2)(T_{\mathrm{w}} + T_{\infty}).$$

Linear(ized) Case: $\tilde{\eta}^{\mathrm{lin}}(T_{\mathrm{lin,c}}, T_{\mathrm{lin,r}})$

$$\tilde{\eta}_{\mathrm{c}}^{\mathrm{lin}} = \langle \bar{\eta}_{\mathrm{c}}^{\mathrm{iso}} \rangle [T_{\mathrm{lin,c}}];\ \tilde{\eta}_{\mathrm{r}}^{\mathrm{lin}} = \varepsilon_{\mathrm{r}} \sigma_{\mathrm{SB}} (T_{\mathrm{lin,r}}^2 + T_{\infty}^2)(T_{\mathrm{lin,r}} + T_{\infty}).$$

where (say) $T_{\mathrm{lin,c}} = T_{\mathrm{lin,r}} = T_{\mathrm{i}}$.

Motivation and Notation

P Phan 2.51

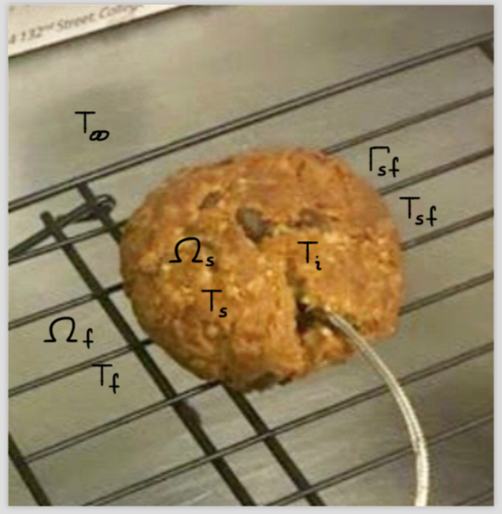

An Idealized Configuration

Let $\Omega \subset \mathbb{R}^3$, $\overline{\Omega} = \overline{\Omega_\mathrm{s}} \cup \overline{\Omega_\mathrm{f}}$:

$\Omega_\mathrm{f} \equiv$ fluid (air) domain: effectively infinite;

$\Omega_\mathrm{s} \equiv$ solid domain: convex, (single, scale) parameter ℓ;

$\Gamma_\mathrm{sf} \equiv \overline{\Omega_\mathrm{s}} \cap \overline{\Omega_\mathrm{f}} \setminus \overline{\Gamma_\mathrm{s}^\mathrm{ad}}$; $\partial\Omega_\mathrm{s} \equiv \overline{\Gamma_\mathrm{sf}} \cup \overline{\Gamma_\mathrm{s}^\mathrm{ad}}$

uniformly large enclosure: $\mathrm{dist}(\Omega_\mathrm{s}, \partial\Omega) \gg \ell$;

coordinate system: $x \equiv (x_1, x_2, x_3)$, $\{\mathbf{e}_i\}_i$; gravity $\mathbf{g} = -g\mathbf{e_2}$.

Initial conditions: $T|_{\Omega_\mathrm{s}} \equiv T_\mathrm{s} = T_\mathrm{i}$ uniform, $T|_{\Omega_\mathrm{f}} \equiv T_\mathrm{f} = T_\infty$;
assume $T_\mathrm{i} > T_\infty$ (wlog).

Farfield conditions: *quiescent* fluid; $T_\mathrm{f} = T_\infty$ (on $\partial\Omega$) — implicit.

Governing Equations: Dimensional linear(ized)

Temperature $T_s(x,t)$ satisfies

$$\frac{\partial T_s}{\partial t} = \alpha_s \nabla^2 T_s \quad \text{in } \Omega_s,\ t > 0\ ,$$

$$\underbrace{-k_s \nabla T_s \cdot \hat{\mathbf{n}}}_{\text{Fourier's Law}} = \underbrace{\tilde{\eta}^{\text{lin}}(T_i, T_i)}_{\text{HTC}}(T_s - T_\infty) \quad \text{on } \partial\Omega_s \equiv \Gamma_{sf},\ t > 0\ ,$$

$$T_s(\cdot, t=0) = T_i \quad \text{in } \Omega_s\ .$$

Dunk pPDE: $\mathbb{M}^{[1]}[\Omega_s^{\text{geo}}]$, geo $\in \{P, C, S\}$

$$\mu^{[1]} \equiv (\text{geo}, \ell, \alpha_s, k_s, \tilde{\eta}^{\text{lin}}, T_\infty, T_i, t_{\text{final}}) \in \mathcal{P}^{[1]}$$
$$\mapsto T_s(x,t), x \in \Omega_s, t \in (0, t_{\text{final}}]; \mathrm{o} = \mathrm{O}^{[1]}(T_s)\,.$$

Here $\mathrm{O}^{[1]}$ is a linear bounded output functional.

Remark Dimensional formulation for expositional convenience.

Governing Equation

Let $\mathrm{Bi}^{dunk} \equiv \dfrac{\tilde{\eta}^{\mathrm{lin}}\,|\Omega_{\mathrm{s}}|}{k_{\mathrm{s}}\,|\Gamma_{\mathrm{sf}}|}$.

For $\mathrm{Bi}^{dunk} \ll 1,\ T_{\mathrm{s}}(x,t) \approx \hat{T}_{\mathrm{s}}(t)$ satisfies

$$\frac{k_{\mathrm{s}}}{\alpha_{\mathrm{s}}}|\Omega_{\mathrm{s}}|\frac{d(\hat{T}_{\mathrm{s}} - T_\infty)}{dt} + \tilde{\eta}^{\mathrm{lin}}\,|\Gamma_{\mathrm{sf}}|(\hat{T}_{\mathrm{s}} - T_\infty) = 0\,,$$

subject to $(\hat{T}_{\mathrm{s}} - T_\infty)(t=0) = (T_{\mathrm{i}} - T_\infty)$.

Dunk pPDE: $\mathbb{M}^{[1]}[-], \mathrm{geo} = \textsc{lumped}$

$$\mu^{[1]} \equiv \big(\mathrm{geo}, |\Omega_{\mathrm{s}}|, |\Gamma_{\mathrm{sf}}|, k_{\mathrm{s}}, \alpha_{\mathrm{s}}, \tilde{\eta}^{\mathrm{lin}}, T_\infty, T_{\mathrm{i}}, t_{\mathrm{final}}\big) \in \mathcal{P}^{[1]}$$
$$\mapsto \hat{T}_{\mathrm{s}}(t), t \in (0, t_{\mathrm{final}}]; \mathrm{o} = \mathtt{O}^{[1]}(\hat{T}_{\mathrm{s}})\,.$$

Here $\mathtt{O}^{[1]}$ is a linear output functional.

Remark pMOR (parametrized Model Order Reduction).

Heat Transfer 101

the *Fin* Problem

Motivation and Notation

An Idealized Configuration

Let $\Omega \subset \mathbb{R}^3$, $\overline{\Omega} = \overline{\Omega_s} \cup \overline{\Omega_f}$:

$\Omega_f \equiv$ fluid domain: effectively of infinite extent, $\partial\Omega_f = \partial\Omega$;

$\Omega_s \equiv$ solid domain: $\overline{\Omega_s} \equiv \overline{\Omega_{s-}}\ (x_1 \leq 0) \cup \overline{\Omega_{s+}}\ (x_1 \geq 0)$;

$\Omega_{s+} \equiv$ Right Cylinder $\{0 < x_1 < L, (x_2, x_3) \in \mathcal{D}_{cs}\}$:

$\mathcal{D}_{cs} \equiv$ cross section: convex; area A_{cs}, perimeter P_{cs};

$\partial\Omega_{s+} \equiv \overline{\Gamma_{sr}} \cup \overline{\Gamma_{sf}} \cup \overline{\Gamma_{st}}$: $\Gamma_{sf} \equiv]0, L[\, \times \partial\mathcal{D}_{cs}$, $P_{cs} L / A_{cs} \gg 1$;

uniformly large enclosure: $\text{dist}(\Omega_s, \partial\Omega) \gg \ell$;

coordinate system: $x \equiv (x_1, x_2, x_3)$, $\{\mathbf{e}_i\}_i$; gravity $\mathbf{g} = -g\mathbf{e}_3$;

Farfield conditions: *quiescent* fluid; $T_f = T_\infty$ (on $\partial\Omega$) — implicit.

Insulated Tip: $-k_s \frac{\partial T_s}{\partial x_1} = 0$ on Γ_{st}, *natural* — implicit.

Temporal Stages

Stage I. Steady-State: $T_s^{ss}(x)$

estimate or measure steady-state temperature over Γ_{sr},

$\overline{T}_{root}$ ($> T_\infty$, wlog) uniform;

predict temperature $T_s^{ss}(x) \equiv T_s(x, t \to \infty), x \in \Omega_{s+}$.

Stage II. Cooldown: $T_s^{cd}(x,t)$

impose zero flux boundary condition on Γ_{sr};

provide initial condition,

$T_s^{cd}(x, t = 0) = T_s^{ss}(x), x \in \Omega_{s+}$ (reset time);

predict temperature $T_s^{cd}(x,t), x \in \Omega_{s+}, t > 0$.

Notation: $\overline{}$ denotes spatial average over cross section.

Governing Equations: Dimensional

Steady-State Stage

Temperature $T_\mathrm{s} \equiv T_\mathrm{s}^\mathrm{ss}(x)$ satisfies

$$-k_\mathrm{s}\nabla^2 T_\mathrm{s} = 0 \text{ in } \Omega_{\mathrm{s}+} \ ,$$

$$\underbrace{-k_\mathrm{s}\nabla T_\mathrm{s}\cdot\hat{\mathbf{n}}}_{\text{Fourier's Law}} = \underbrace{\tilde{\eta}^\mathrm{lin}(\overline{T}_\mathrm{root}, \overline{T}_\mathrm{root})}_{\text{HTC}}(T_\mathrm{s} - T_\infty) \text{ on } \Gamma_\mathrm{sf} \ ,$$

$$T_\mathrm{s} = \overline{T}_\mathrm{root} \text{ on } \Gamma_\mathrm{sr} \ ,$$

$$-k_\mathrm{s}\nabla T_\mathrm{s}\cdot\hat{\mathbf{n}} = 0 \text{ (insulated tip) on } \Gamma_\mathrm{st} \ .$$

Cooldown Stage: incorporate $\dfrac{\partial T_\mathrm{s}}{\partial t}$ and initial condition T_s^ss.

Governing Equations: Dimensional

Let $\mathrm{Bi}^{\mathrm{fin}} \equiv \dfrac{\tilde{\eta}^{\mathrm{lin}} A_{\mathrm{cs}}}{k_{\mathrm{s}} P_{\mathrm{cs}}}$.

For $\mathrm{Bi}^{\mathrm{fin}} \ll 1$, $\dfrac{P_{\mathrm{cs}} L}{A_{\mathrm{cs}}} \gg 1$, $T_{\mathrm{s}}(x) \approx \hat{T}_{\mathrm{s}}(x_1)$ satisfies

$$-k_{\mathrm{s}} A_{\mathrm{cs}} \frac{d(\hat{T}_{\mathrm{s}} - T_\infty)}{dx_1^2} + \eta^{\mathrm{lin}} P_{\mathrm{cs}} (\hat{T}_{\mathrm{s}} - T_\infty) = 0\,, 0 < x_1 < L\,,$$

$$\hat{T}_{\mathrm{s}} = \overline{T}_{\mathrm{root}} \text{ at } x_1 = 0\,,\ -k_{\mathrm{s}} \frac{d(\hat{T}_{\mathrm{s}} - T_\infty)}{dx_1} = 0 \text{ at } x_1 = L\,.$$

Fin pPDE: $\mathbb{M}^{[2]}$

$$\mu^{[2]} \equiv \left(k_{\mathrm{s}}, A_{\mathrm{cs}}, P_{\mathrm{cs}}, \tilde{\eta}^{\mathrm{lin}}, T_\infty\right) \in \mathcal{P}^{[2]}$$
$$\mapsto \hat{T}_{\mathrm{s}}(x_1), 0 \le x_1 \le L; \mathrm{o} = \mathrm{O}^{[2]}(\hat{T}_{\mathrm{s}})\,.$$

Here $\mathrm{O}^{[2]}$ is a linear output functional.

Weak Form

Let $X^{\mathrm{E}} = \{v \in H^1(\Omega_{\mathrm{s}+}) \,|\, v|_{\Gamma_{\mathrm{sr}}} = \overline{T}_{\mathrm{root}}\}$

$X \;\; = \{v \in H^1(\Omega_{\mathrm{s}+}) \,|\, v|_{\Gamma_{\mathrm{sr}}} = 0\}.$

Then $T_{\mathrm{s}} \in X^{\mathrm{E}}$ satisfies

$$\int_{\Omega_{\mathrm{s}+}} k_{\mathrm{s}} \nabla (T_{\mathrm{s}} - T_\infty) \cdot \nabla v + \eta^{\mathrm{lin}} \int_{\Gamma_{\mathrm{sf}}} (T_{\mathrm{s}} - T_\infty) v = 0\,,\ \forall v \in X\,.$$

Let $\hat{X}^{\mathrm{E}} = \{v \in X^{\mathrm{E}} \,|\, v \text{ function of } x_1 \text{ only}\} \subset X^{\mathrm{E}}$

$\hat{X} \;\; = \{v \in X \;\,|\, v \text{ function of } x_1 \text{ only}\} \subset X\,.$

Find $\hat{T}_{\mathrm{s}} \in \hat{X}^{\mathrm{E}}$ such that optimal in energy norm

$$\int_{\Omega_{\mathrm{s}+}} k_{\mathrm{s}} \nabla (\hat{T}_{\mathrm{s}} - T_\infty) \cdot \nabla v + \tilde{\eta}^{\mathrm{lin}} \int_{\Gamma_{\mathrm{sf}}} (\hat{T}_{\mathrm{s}} - T_\infty) v = 0\,,\ \forall v \in \hat{X}.$$

Weak Form

Let $X^{\mathrm{E}} = \{v \in H^1(\Omega_{\mathrm{s}+}) \,|\, v|_{\Gamma_{\mathrm{sr}}} = \overline{T}_{\mathrm{root}}\}$

$X \;\; = \{v \in H^1(\Omega_{\mathrm{s}+}) \,|\, v|_{\Gamma_{\mathrm{sr}}} = 0\}$.

Then $T_{\mathrm{s}} \in X^{\mathrm{E}}$ satisfies

$$\int_{\Omega_{\mathrm{s}+}} k_{\mathrm{s}} \nabla (T_{\mathrm{s}} - T_\infty) \cdot \nabla v + \eta^{\mathrm{lin}} \int_{\Gamma_{\mathrm{sf}}} (T_{\mathrm{s}} - T_\infty) v = 0\,, \; \forall v \in X\,.$$

Let $\hat{X}^{\mathrm{E}} = \{v \in X^{\mathrm{E}} \,|\, v \text{ function of } x_1 \text{ only}\} \subset X^{\mathrm{E}}$

$\hat{X} \;\; = \{v \in X \;\, |\, v \text{ function of } x_1 \text{ only}\} \subset X\,.$

Find $\hat{T}_{\mathrm{s}} \in \hat{X}^{\mathrm{E}}$ such that optimal in energy norm

$$k_{\mathrm{s}} A_{\mathrm{cs}} \int_0^L \frac{d(\hat{T}_{\mathrm{s}} - T_\infty)}{dx_1} \frac{dv}{dx_1}\, dx_1 + \tilde{\eta}^{\mathrm{lin}} P_{\mathrm{cs}} \int_0^L (\hat{T}_{\mathrm{s}} - T_\infty) v \, dx_1 = 0, \; \forall v \in \hat{X}.$$

Heat Transfer Back-of-the Envelope (BE) Framework

Formulation

General Form

Given

solid artifact A from *set of artifacts* (or natural objects);

environment;

environment conditions E from *set of environment conditions*;

process applied to artifact;

process conditions P from *set of process conditions*;

output operator O: $X(\Omega_s^{\mathtt{A}}) \to Y$;

provide

numeric estimate for output, $o^{est} \approx \mathtt{O}(T_s^{phy}(\mathtt{A},\mathtt{E},\mathtt{P}))$

quantitative justification for proposed answer. SHOW YOUR WORK

Remark Problem Statement is *non-prescriptive*.

General Form

Given TEACHER

solid artifact A from *set of artifacts* (or natural objects);

environment;

environment conditions E from *set of environment conditions*;

process applied to artifact;

process conditions P from *set of process conditions*;

output operator O: $X(\Omega_{\mathrm{s}}^{\mathtt{A}}) \to Y$;

provide

numeric estimate for output, $\mathrm{o}^{\mathrm{est}} \approx \mathtt{O}(T_{\mathrm{s}}^{\mathrm{phy}}(\mathtt{A},\mathtt{E},\mathtt{P}))$

quantitative justification for proposed answer. SHOW YOUR WORK

Remark Problem Statement is *non-prescriptive*.

General Form

Given TEACHER

solid artifact A from *set of artifacts* (or natural objects);

environment;

environment conditions E from *set of environment conditions*;

process applied to artifact;

process conditions P from *set of process conditions*;

output operator O: $X(\Omega_{\mathrm{s}}^{\mathtt{A}}) \to Y$;

provide STUDENT: BE Single-Screen Script

numeric estimate for output, $\mathrm{o}^{\mathrm{est}} \approx \mathtt{O}(T_{\mathrm{s}}^{\mathrm{phy}}(\mathtt{A},\mathtt{E},\mathtt{P}))$

quantitative justification for proposed answer. SHOW YOUR WORK

Remark Problem Statement is *non-prescriptive*.

Summary

1. Material property function: material $\mapsto k_{\mathsf{s}}, \alpha_{\mathsf{s}}, k_{\mathsf{f}}, \alpha_{\mathsf{f}}, \nu, \beta, \varepsilon_{\mathsf{r}}$.

2. Set of *convection heat transfer coefficient* ($\mathsf{HTC_c}$) functions

$$\mathbb{S}_{\mathsf{HTC_c}} \equiv \{\text{Plate}(\theta_g), \text{Circular Cylinder}, \text{Sphere}\}$$

for forced and natural convection.

3. Set of *radiation heat transfer coefficient* ($\mathsf{HTC_r}$) functions

$$\mathbb{S}_{\mathsf{HTC_r}} \equiv \{\text{Parallel Plates}, \text{Convex Body in Enclosure}\}$$

for graybody heat exchange.

4. Set of pPDE models

$$\mathbb{S}_{\mathsf{pPDEs}} \equiv \{\mathbb{M}^{[1]}, \mathbb{M}^{[2]}, \mathbb{M}^{[3]}, \mathbb{M}^{[4]}\}$$

for heat transfer in solid body in communication with environment.

Summary

1. Material property function: material $\mapsto k_\mathsf{s}, \alpha_\mathsf{s}, k_\mathsf{f}, \alpha_\mathsf{f}, \nu, \beta, \varepsilon_\mathsf{r}$.

2. Set of *convection heat transfer coefficient* ($\mathsf{HTC_c}$) functions

$$\mathbb{S}_{\mathsf{HTC_c}} \equiv \{\mathsf{Plate}(\theta_g), \mathsf{Circular\ Cylinder}, \mathsf{Sphere}\}$$

for forced and natural convection. Nu(sselt) pPDE models

3. Set of *radiation heat transfer coefficient* ($\mathsf{HTC_r}$) functions

$$\mathbb{S}_{\mathsf{HTC_r}} \equiv \{\mathsf{Parallel\ Plates}, \mathsf{Convex\ Body\ in\ Enclosure}\}$$

for graybody heat exchange.

4. Set of pPDE models

$$\mathbb{S}_{\mathsf{pPDEs}} \equiv \{\mathbb{M}^{[1]}, \mathbb{M}^{[2]}, \mathbb{M}^{[3]}, \mathbb{M}^{[4]}\}$$

for heat transfer in solid body in communication with environment.

$\mathbb{S}_{\mathrm{pPDEs}}$: Set of pPDEs

$\mathbb{M}^{[1]}$: *Dunk(ing)*

$$\mathbb{M}^{[1]}[-] \qquad \mathrm{geo} = \text{LUMPED}\,; \qquad \mathrm{Bi}^{\mathrm{dunk}} \ll 1$$

$$\mathbb{M}^{[1]}[\Omega_s^P] \qquad \mathrm{geo} = P \;:\Omega_s^P \equiv]-\ell,\ell[\times\mathcal{D}^{\mathrm{ad}}\,;$$

$$\mathbb{M}^{[1]}[\Omega_s^C] \qquad \mathrm{geo} = C : \Omega_s^C \equiv \{(x_1^2 + x_2^2) < \ell^2\} \times \mathcal{D}^{\mathrm{ad}}\,;$$

$$\mathbb{M}^{[1]}[\Omega_s^S] \qquad \mathrm{geo} = S \;: \Omega_s^S \equiv \{(x_1^2 + x_2^2 + x_3^2) < \ell^2\}\,.$$

$\mathbb{M}^{[2]}$: *Fin* . $\qquad \mathrm{Bi}^{\mathrm{fin}} \ll 1$

$\mathbb{M}^{[3]}$: *Wall* .

$\mathbb{M}^{[4]}$: *Semi-Infinite Body* .

Remark PDE complexity: IBVP in time and *one* spatial coordinate.

Transformation Framework No Composition

Given PS, define *notional* "truth" PDE model:

$$\mathbb{M}^{\mathrm{PS}} : (\mathtt{A},\mathtt{E},\mathtt{P}) \mapsto \Omega_s^{\mathtt{A}},\, T_{\mathrm{s}}^{\mathrm{phy}}, \mathrm{o}^{\mathrm{phy}} = \mathtt{O}(T_{\mathrm{s}}^{\mathrm{phy}});$$

in general, $\mathbb{M}^{\mathrm{PS}}$ can not (certainly will not) be evaluated.

Notation: $^{\mathrm{phy}}$ denotes noise-free measurement of physical artifact.

Transformation Framework — No Composition

Given PS, define *notional* "truth" PDE model:

$$\mathbb{M}^{\mathsf{PS}} : (\mathtt{A},\mathtt{E},\mathtt{P}) \mapsto \Omega_s^{\mathtt{A}},\, T_{\mathsf{s}}^{\mathsf{phy}}, \mathsf{o}^{\mathsf{phy}} = \mathtt{O}(T_{\mathsf{s}}^{\mathsf{phy}});$$

in general, $\mathbb{M}^{\mathsf{PS}}$ can not (certainly will not) be evaluated.

Notation: $^{\mathsf{phy}}$ denotes noise-free measurement of physical artifact.

Choose

$\bar{n} \in \{1, \ldots, 4\}$: a pPDE $\mathbb{M}^{[\bar{n}]} \in \mathbb{S}_{\mathsf{pPDEs}}$ model selection

$\bar{\mu}^{[\bar{n}]} \in \mathcal{P}^{[\bar{n}]}$ associated to $\mathbb{M}^{[\bar{n}]}$ parameter selection

such that

$$\mathsf{o}^{\mathsf{est}} \equiv \mathsf{o}^{[\bar{n}]} = \mathtt{O}^{[\bar{n}]}(T_{\mathsf{s}}^{[\bar{n}]}(\bar{\mu}^{[\bar{n}]})) \approx \mathsf{o}^{\mathsf{phy}};$$

or declare that Problem Statement is "outside envelope."

Transformation Framework — No Composition

Given PS, define *notional* "truth" PDE model:

$$\mathbb{M}^{\mathrm{PS}} : (\mathtt{A},\mathtt{E},\mathtt{P}) \mapsto \Omega_s^{\mathtt{A}},\ T_{\mathrm{s}}^{\mathrm{phy}}, \mathrm{o}^{\mathrm{phy}} = \mathtt{O}(T_{\mathrm{s}}^{\mathrm{phy}});$$

in general, $\mathbb{M}^{\mathrm{PS}}$ can not (certainly will not) be evaluated.

Notation: $^{\mathrm{phy}}$ denotes noise-free measurement of physical artifact.

Choose

$\bar{n} \in \{1, \ldots, 4\}$: a pPDE $\mathbb{M}^{[\bar{n}]} \in \mathbb{S}_{\mathrm{pPDEs}}$ model selection

$\bar{\mu}^{[\bar{n}]} \in \mathcal{P}^{[\bar{n}]}$ associated to $\mathbb{M}^{[\bar{n}]}$ parameter selection

such that

$$\mathrm{o}^{\mathrm{est}} \equiv \mathrm{o}^{[\bar{n}]} = \mathtt{O}^{[\bar{n}]}(T_{\mathrm{s}}^{[\bar{n}]}(\bar{\mu}^{[\bar{n}]})) \approx \mathrm{o}^{\mathrm{phy}};$$

or declare that Problem Statement is "outside envelope."

Approach: classification PS $(\mathtt{A},\mathtt{E},\mathtt{P},\mathtt{O}) \mapsto \bar{n}, \mathbb{M}^{[\bar{n}]}$ preliminary;
simplification $\mathbb{M}^{\mathrm{PS}} \mapsto \mathbb{M}^{[\bar{n}]}(\bar{\mu}^{[\bar{n}]})$ and confirm $\bar{n}$.

Techniques

Replace Conjugate Framework with Classical Framework.

Modify

- Geometry
- Materials and Thermophysical Properties
- Initial and Boundary Conditions
- Heat Transfer Coefficients: $\mathrm{HTC_c}$, $\mathrm{HTC_r}$.

Apply (Parametrized) Model Order Reduction

— Dimensional*ity* Reduction

Justifications

Invoke PDE (and domain) knowledge:

- order-of-magnitude estimates,
- stability and perturbation results,
- asymptotic analysis,
- closed-form solutions,
- approximation theory,
- variational methods,
- computational studies,
- experimental observations,

often with sign information for $(\mathrm{o}^{\mathrm{est}} - \mathrm{o}^{\mathrm{phy}})$.

Requirements $\rightarrow$ Objectives and Applications

BE Instruction Set functions are shared by large community:

continual verification.

BE Instruction Set functions are encapsulated:

blunder prevention.

BE Instruction Set functions are fast:

rapid response for design and optimization.

BE Code is transparent:

assessment of proposed output estimate, o^{est};

blunder detection.

Requirements → Objectives and Applications

BE Instruction Set functions are shared by large community:

continual verification.

BE Instruction Set functions are encapsulated:

blunder prevention.

BE Instruction Set functions are fast:

rapid response for design and optimization.

BE Code is transparent:

assessment of proposed output estimate, o^{est};

blunder detection within BE Code.

Requirements $\rightarrow$ Objectives and Applications

BE Instruction Set functions are shared by large community:

continual verification.

BE Instruction Set functions are encapsulated:

blunder prevention.

BE Instruction Set functions are fast:

rapid response for design and optimization.

BE Code is transparent:

assessment of proposed output estimate, o^{est};

blunder detection of large-scale simulation.

Heat Transfer
Back-of-the-Envelope Framework

Examples of Parameter Selection:
Truth Model Simplification

Artifact and Environment

E Miller 2.51

Artifact: Bagelhalf

Environment: Kitchen; $T_\infty \approx 20°\text{C}$.

Remark Proximity of bagelhalf to back wall.

Process and Outputs

Process:

1. Remove Bagelhalf from toaster.
2. Place Bagelhalf on cooling rack in vertical orientation.
3. Measure Bagelhalf (mid-radius) surface temperature:

$$T_{\text{surface}}^{\text{Bagelhalf}}(t=0) \equiv T_{\text{i}} \approx 135^{\circ}\text{C}.$$

Output:

Temperature $T_{\text{surface}}^{\text{Bagelhalf}}(t), t > 0.$

Validation Experiment:

Measure with IR thermometer $T_{\text{surface}}^{\text{Bagelhalf}}(t), t > 0.$

Key Simplifications

Modifications to Truth PDE: Conjugate $\rightarrow$ Classical

Geometry: $\Omega_\mathrm{s} \equiv \,]-\ell, \ell[\times \mathcal{D}$; $\mathcal{D} \equiv]0, L_\mathrm{horiz}[\times]0, L_\mathrm{vert}[$.

Justification: material addition small in relevant metrics.

Boundary Conditions: lateral surfaces $]-\ell, \ell[\times \partial\mathcal{D}$ *insulated*.

Justification: large aspect ratio.

Regime: $\mathrm{Bi}^\mathrm{dunk} \approx 0.5$ *not small*:

apply $\mathbb{M}^{[1]}[\Omega_\mathrm{s}^{\mathrm{geo}=P\mathrm{arallelepiped}}]$ — $\mathrm{IBVP}(x_1, t)$.

Convection HTC: Vertical Plates, $L_\mathrm{eff} = L_\mathrm{vert}$; $T_\mathrm{lin,c} = T_\mathrm{i}$.

Radiation HTC: Convex graybody in enclosure; $\varepsilon_\mathrm{r} = 0.96$;

$T_\mathrm{lin,r} = T_\mathrm{i}$ (UB); $T_\mathrm{lin,r} = T_\infty$ (LB);.

Simplified Geometry

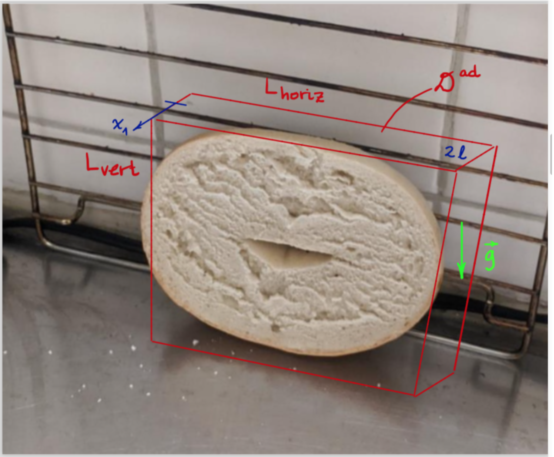

Surface Temperature

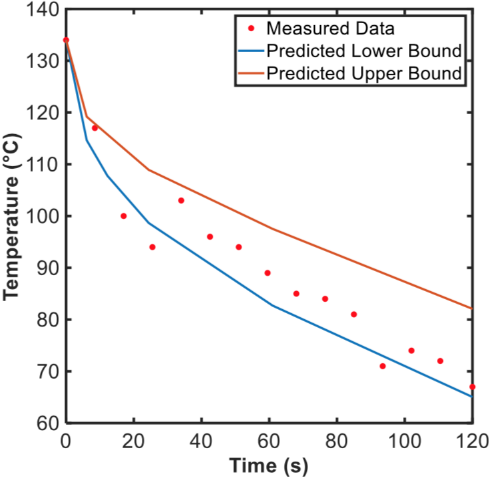

Artifact: Cast-Iron Skillethandle

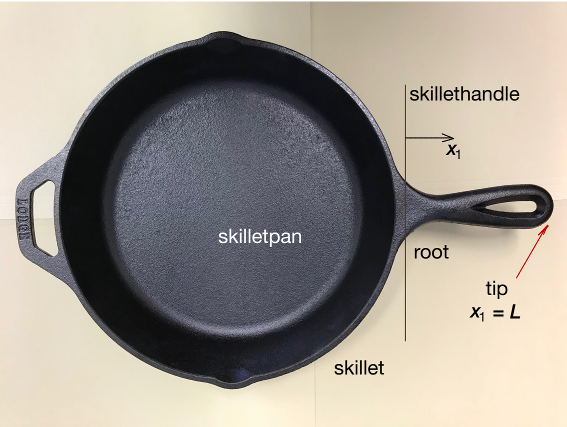

Artifact: Chamfer Details

Remark Sharp corners: (weak) singularities.

Artifact: Cross Section Area and Perimeter

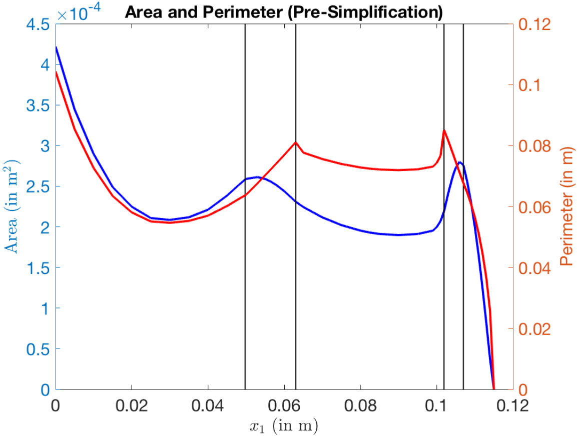

Environment: James Penn's Kitchen

Elements:

- Gas Range
- Cork Trivet on Chair
- IR Camera Jig
- Roomwalls

Temperature of room and roomwalls, $T_\infty \approx 22.6^\circ\mathrm{C}$.

Process

Sequence of steps:

Stage I: Steady-State

1. Boil water in skilletpan until reach steady state.
2. Remove water from skillet pan, and immediately...
3. Measure (or estimate)
   temperature at skillethandle root, $\overline{T}_{\text{root}} \approx 78.6°\text{C}$.

Stage II: Cooldown

4. Place skillet on trivet.

Outputs

Stage I: Steady-Stage

Skillethandle temperature at $t = 0$:

$$\overline{T}_{\mathrm{s}}^{\mathrm{ss}}(x_1), 0 \le x_1 \le L.$$

Stage II: Cooldown

Skillethandle root temperature for $t > 0$:

$$\overline{T}_{\mathrm{root}}^{\mathrm{cd}}(t) = \overline{T}_{\mathrm{s}}^{\mathrm{cd}}(x_1 = 0, t).$$

Skillethandle tip temperature for $t > 0$:

$$\overline{T}_{\mathrm{tip}}^{\mathrm{cd}}(t) = \overline{T}_{\mathrm{s}}^{\mathrm{cd}}(x_1 = L, t).$$

Key Simplifications

Modifications to Truth PDE: Conjugate $\rightarrow$ Classical

Geometry: $\Omega_{s+} \equiv$ right cylinder of *circular* cross section:

$$A_{cs} \equiv \frac{1}{L}\int_0^L \text{Area}(x_1)dx_1\,,\; P_{cs} \equiv \frac{1}{L}\int_0^L \text{Peri}(x_1)dx_1\,.$$

Justification: material modification small in relevant metrics.

Regime: $\text{Bi}^{\text{fin}} \ll 1$, $P_{cs}L/A_{cs} \gg 1$: apply $\mathbb{M}^{[2]}$.

Convection HTC: Horizontal Cylinder 2-D; $D = D_{\text{eff}} \equiv P_{cs}/\pi$.

Justification: D_{eff} preserves boundary-layer length;

$\delta^{\text{bl}} \approx \ell/\langle\overline{\text{Nu}}_D\rangle \ll$ fin axial length scale.

Radiation HTC: Convex graybody in enclosure; $\varepsilon_r = 0.95$.

Justification: blackbody convex-hull equivalence result.

Validation Temperature Measurements $t = 0$ (Stage I)

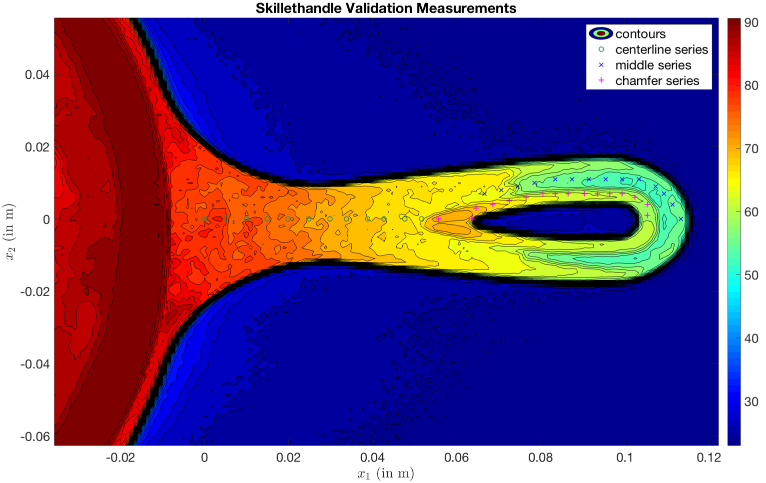

Accuracy: Steady State $\qquad \varepsilon_{\rm r} = 0.95$

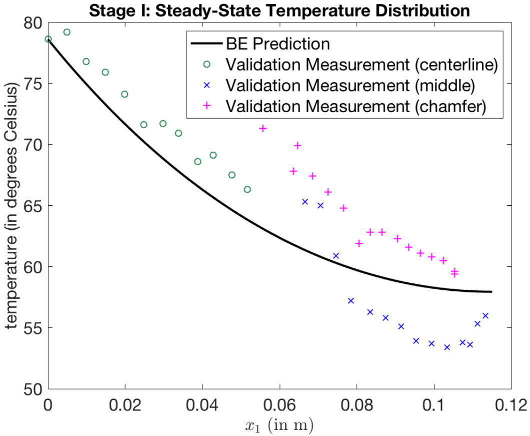

Numerical error: [53]

$$\| T_{\rm s} - T_{\rm s}^h \|_{L^\infty(\Omega_{\rm s})} \le 0.0001 \text{ (\textit{a posteriori} indicator).}$$

Sensitivity to Emissivity $\varepsilon_r = 0.50$

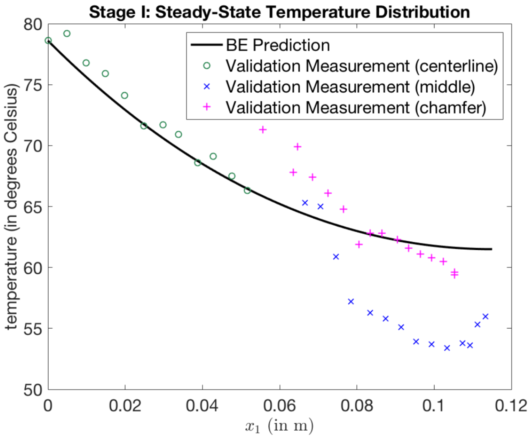

Accuracy: Cooldown

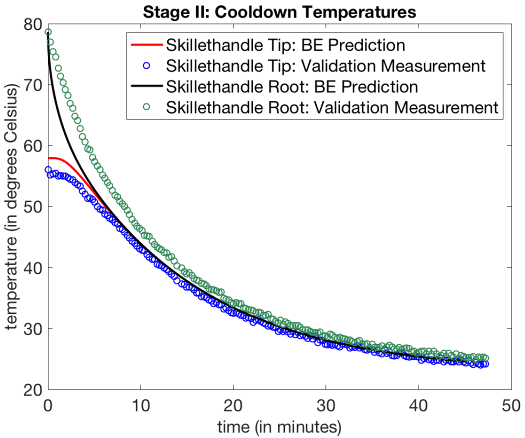

Parametrized Model Order Reduction: Reduced Basis Method [27, 47]

Nusselt Number: Slot Flow

P-H Tsai, Fischer Group, UIUC

Motivation: Trombe Wall

M Kessler 2.51

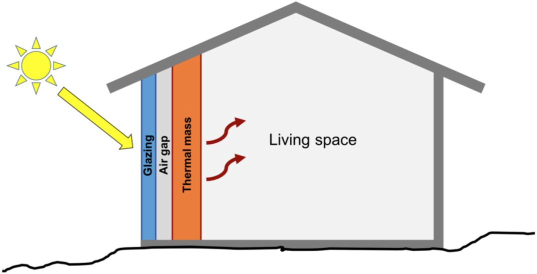

Figure 1: Trombe wall design. Sunlight passes through glazing and warms an air layer. Heat is transferred through a thermal mass made of high heat capacity material and into the living space.

pPDE *Wall*: Parallel Thermal Resistances in Series

Nusselt Configuration: Air Gap — Idealized [46]

Spatial domain: $\Omega_{\mathrm{f}} \equiv]-\ell/2, \ell/2[\times]-10\ell, 10\ell[\subset \mathbb{R}^2$;

$$\Omega_{\mathrm{f}}^* \equiv]-1/2, 1/2[\times]10, 10[.$$

Boundary conditions (nondimensional):

$\Theta_{\mathrm{f}} = -1$ at $x_1^* = -1/2$ and $\Theta_{\mathrm{f}} = 1$ at $x_1^* = 1/2$;

insulated on $x_2^* = -10$ and $x_2^* = 10$.

Variable angle of gravity, $\theta_g \in \mathcal{P}_{\theta_g} \equiv [0, 180°]$:

$$\text{buoyancy force } \Theta_{\mathrm{f}} \left(-\mathbf{e}_1 \cos\theta_{\mathrm{g}} + \mathbf{e}_2 \sin\theta_{\mathrm{g}}\right).$$

Nusselt number: $\langle \overline{\mathrm{Nu}}_\ell \rangle \equiv \langle \dfrac{1}{2\cdot 20} \displaystyle\int_{-10}^{10} \dfrac{\partial \Theta_{\mathrm{f}}}{\partial x_1^*}\Big|_{x_1^* = -\frac{1}{2}} \, dx_2^* \rangle$.

Parameter variation:

$$\langle \overline{\mathrm{Nu}}_\ell \rangle = \langle \overline{\mathrm{Nu}}_\ell \rangle(\theta_g; \mathrm{Ra}_\ell, \mathrm{Pr}); \ \mathrm{Ra}_\ell = 10^3, \ \mathrm{Pr} = 0.71.$$

Governing Equations: Nondimensional Nusselt pPDE

Find $[V^* \equiv (V_1^*, V_2^*, V_3^*), \Theta_f](x^*, t^*)$ $\quad \Theta_f(\cdot, t^* = 0) = 0$ in Ω_f^*

$$\frac{\partial V^*}{\partial t^*} + V^* \cdot \nabla V^* = -\nabla p^* + \mathrm{Pr}^{\frac{1}{2}} (\mathrm{Ra}_\ell^{\mathrm{w}})^{-\frac{1}{2}} \, \nabla^2 V^*$$

$$+ \Theta_f(-\mathbf{e}_1 \cos\theta_g + \mathbf{e}_2 \sin\theta_g) \text{ in } \Omega_f^*, t^* > 0 \, ,$$

$$\nabla \cdot V^* = 0 \text{ in } \Omega_f^*, t^* > 0 \, ,$$

$$\frac{\partial \Theta_f}{\partial t^*} + V^* \cdot \nabla \Theta_f = \mathrm{Pr}^{-\frac{1}{2}} (\mathrm{Ra}_\ell^{\mathrm{w}})^{-\frac{1}{2}} \, \nabla^2 \Theta_f \text{ in } \Omega_f^*, t^* > 0 \, ,$$

$$\Theta_f = \pm 1 \text{ at } x_1^* = \pm 1/2 \text{ and } \frac{\partial \Theta_f}{\partial n} = 0 \text{ on } x_2^* = \pm 10, t^* > 0.$$

Evaluate $\langle \overline{\mathrm{Nu}_\ell} \rangle \equiv \langle \frac{1}{2 \cdot 20} \int_0^{20} \frac{\partial \Theta_f}{\partial x_1^*} \Big|_{x_1^* = 0} \, dx_2^* \rangle$.

$\mathrm{Ra}_\ell = 10^3$: Steady States — Current Work

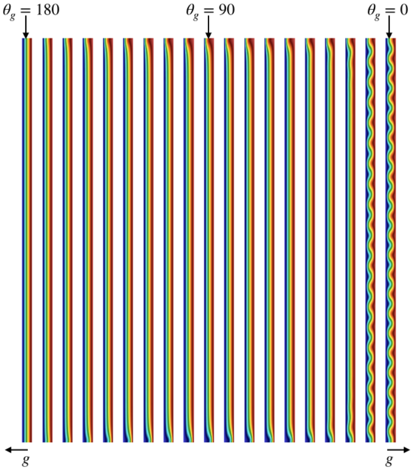

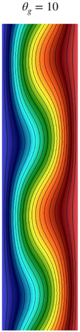

$\mathrm{Ra}_\ell = 10^4$: Statistically Stationary States — Future Work

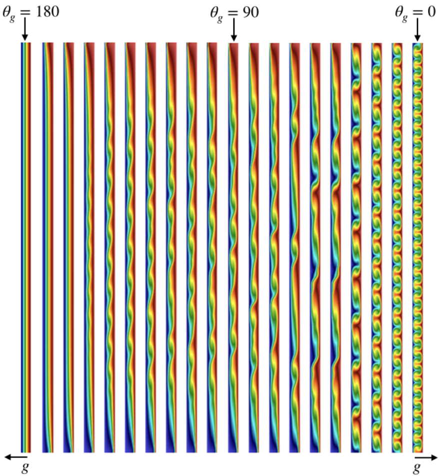

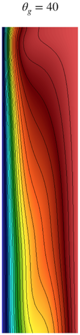

Direct Simulation

Hardware (2-D) 8 processors:

Intel(R) Xeon(R) CPU E5-2620 v3 @ 2.40GHz.

Software Nek5000 parallel spectral element code [43, 16].

Computation Time (Wall-Clock)

2-D Spatial Domain, $\Omega_{\mathrm{f}}^* \equiv]-1/2, 1/2[\times[-10, 10[$:

$\approx$ 1.7s per C(onvective)T(ime)U(nit)s;

$\approx$ 1000 CTU to reach (statistically) stationary state.

Direct Simulation

Hardware (3-D) 64 processors:

Intel(R) Xeon Phi(TM) CPU 7210 @ 1.30GHz.

Software Nek5000 parallel spectral element code [43, 16].

Computation Time (Wall-Clock)

2-D Spatial Domain, $\Omega_{\mathrm{f}}^{*} \equiv]-1/2, 1/2[\times[-10, 10[$:

$\approx$ 1.7s per C(onvective)T(ime)U(nit)s;

$\approx$ 1000 CTU to reach (statistically) stationary state.

3-D Spatial Domain, $\Omega_{\mathrm{f}}^{*} \equiv]-1/2, 1/2[\times]-10, 10[\times]-10, 10[$:

$\approx$ 5000s per CTU;

$\approx$ 1000 CTU to reach (statistically) stationary state.

Parametric Manifold Steady-State

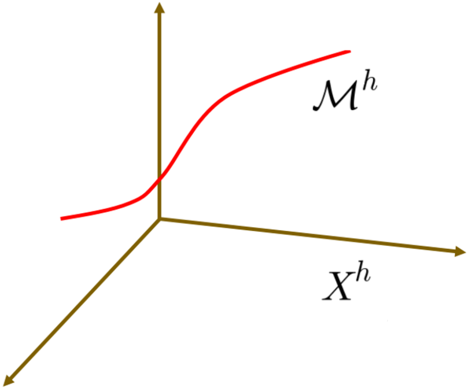

$$[V^*, \Theta_f]^h \in X^h \text{ high-dimensional } \subset X(\Omega_f^*)$$

Parametric Manifold Steady-State

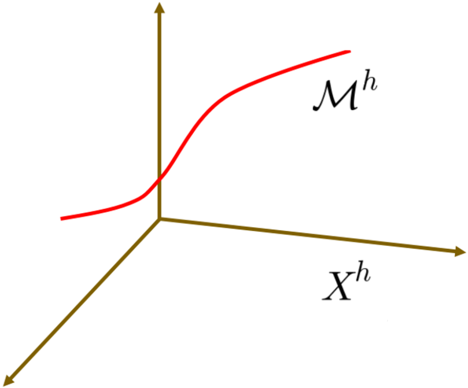

$$[V^*, \Theta_\mathrm{f}]^h \in X^h \text{ high-dimensional } \subset X(\Omega_\mathrm{f}^*)$$

$$[V^*, \Theta_\mathrm{f}]^h \in \mathcal{M}^h \equiv \{[V^*, \Theta_\mathrm{f}]^h(\theta_g) \,|\, \theta_g \in \mathcal{P}_{\theta_g}\}$$

Manifold Snapshots Steady-State

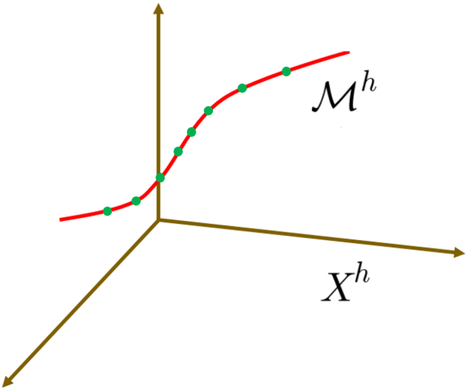

Snapshots: $\xi^m \equiv [V^*, \Theta_{\mathrm{f}}]^h(\hat{\theta}_g^m \in \mathcal{P}_{\theta_g}), m = 1, \ldots, M$.

$\mathrm{Ra}_\ell = 10^3$: Nek5000, $t^* \to \infty$; stable steady states.

Bare Necessities

RB Spaces (hierarchical):

$$X_{\text{RB}}^N \subset \text{span}\{\xi^m, m = 1, \ldots, M\}, 1 \leq N \leq N_{\max}.$$

Weak-Greedy [54] or Proper Orthogonal Decomposition (POD)

Galerkin Projection: $\theta_g \in \mathcal{P}_{\theta_g} \to [V^*, \Theta_{\text{f}}]_{\text{RB}}^N(\theta_g) \in X_{\text{RB}}^N$.

A Posteriori Error Indicator: [54, 14]

$$\|[V^*, \Theta_{\text{f}}]^h - [V^*, \Theta_{\text{f}}]_{\text{RB}}^N\|_X \lesssim \approx \frac{1}{\beta_{\text{inf sup}}^{h\,\text{est}}} \|\text{ residual}^h \|_{X_h'}\,.$$

Affine Expansion in Functions of Parameter:

$$\mathcal{A}_0[V^*, \Theta_{\text{f}}] + \cos(\theta_g)\mathcal{A}_1[V^*, \Theta_{\text{f}}] + \sin(\theta_g)\mathcal{A}_2[V^*, \Theta_{\text{f}}] = \mathcal{F} \in X'\,.$$

Offline-Online Decomposition:

Online complexity *independent* of $\dim(X^h)$.

Bare Necessities

RB Spaces (hierarchical):

$$X_{\mathrm{RB}}^N \subset \mathrm{span}\{\xi^m, m = 1, \ldots, M\}, 1 \leq N \leq N_{\max}.$$

Weak-Greedy [54] or Proper Orthogonal Decomposition (POD)

Galerkin Projection: $\theta_g \in \mathcal{P}_{\theta_g} \to [V^*, \Theta_{\mathrm{f}}]_{\mathrm{RB}}^N(\theta_g) \in X_{\mathrm{RB}}^N$.

A Posteriori Error Indicator: [54, 14]

$$\|[V^*, \Theta_{\mathrm{f}}]^h - [V^*, \Theta_{\mathrm{f}}]_{\mathrm{RB}}^N\|_X \lessapprox \frac{1}{\beta_{\text{inf sup}}^{h\,\text{est}}} \|\text{ residual}^h\|_{X_h'}\,.$$

Affine Expansion in Functions of Parameter:

$$\mathcal{A}_0[V^*, \Theta_{\mathrm{f}}] + \cos(\theta_g)\mathcal{A}_1[V^*, \Theta_{\mathrm{f}}] + \sin(\theta_g)\mathcal{A}_2[V^*, \Theta_{\mathrm{f}}] = \mathcal{F} \in X'\,.$$

Offline-Online Decomposition: real-time, many-query contexts

Online complexity *independent* of $\dim(X^h)$.

Bare Necessities

RB Spaces (hierarchical):

$$X_{\mathrm{RB}}^N \subset \mathrm{span}\{\xi^m, m = 1, \ldots, M\}, 1 \leq N \leq N_{\max}.$$

Weak-Greedy [54] or Proper Orthogonal Decomposition (POD)

Galerkin Projection: $\theta_g \in \mathcal{P}_{\theta_g} \to [V^*, \Theta_{\mathrm{f}}]_{\mathrm{RB}}^N(\theta_g) \in X_{\mathrm{RB}}^N$.

A Posteriori Error Indicator: [54, 14]

$$\|[V^*, \Theta_{\mathrm{f}}]^h - [V^*, \Theta_{\mathrm{f}}]_{\mathrm{RB}}^N\|_X \lessapprox \frac{1}{\beta_{\mathrm{inf\ sup}}^{h\ \mathrm{est}}} \| \text{ residual}^h \|_{X_h'} .$$

Affine Expansion in Functions of Parameter:

$$\mathcal{A}_0[V^*, \Theta_{\mathrm{f}}] + \cos(\theta_g)\mathcal{A}_1[V^*, \Theta_{\mathrm{f}}] + \sin(\theta_g)\mathcal{A}_2[V^*, \Theta_{\mathrm{f}}] = \mathcal{F} \in X' .$$

Offline-Online Decomposition: BE $\mathrm{HTC_c}$ Functions

Online complexity *independent* of $\dim(X^h)$.

Accuracy: POD Bifurcation [26]

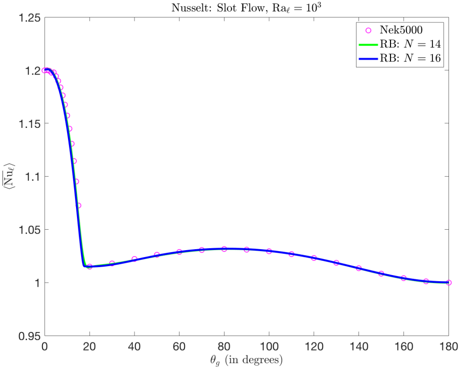

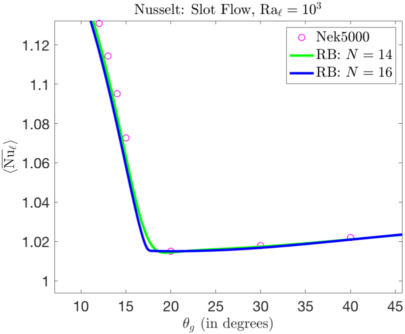

RB: $N = 14$, $N = 16$ ($\leftarrow$ POD spectrum); Newton continuation.

Accuracy: Weak Greedy

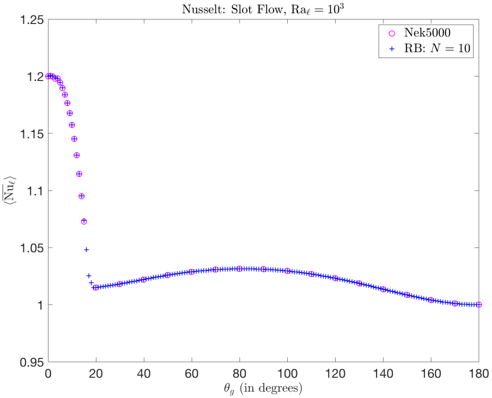

RB: Newton iteration; initialization $\Pi^{X^N_{\mathrm{RB}}}_{H^1(\Omega)}$ of nearest-θ_g snapshot; wall-clock time 4.5ms per θ_g value $\rightarrow \mathbb{S}_{\mathrm{HTC_c}}$.

$\mathrm{Ra}_\ell = 10^4$: Statistically Stationary States [23, 24][55, 21]

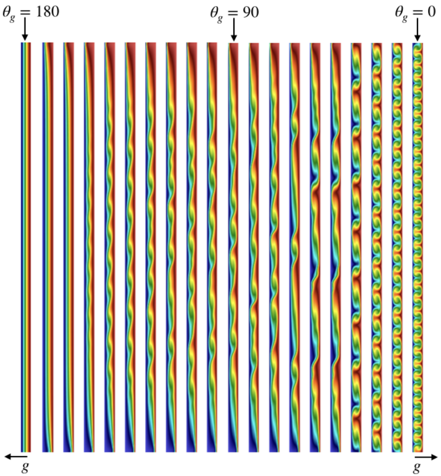

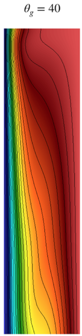

Parametrized Model Order Reduction: Port-Reduced Reduced-Basis Component

Library Thermal Heatsink

L Nguyen, Akselos SA

Parametrized Model Order Reduction: PR-RBC

Library Thermal Heatsink
L Nguyen, Akselos SA

Acoustics Waveguide

Consider a waveguide $\mathcal{D}_\perp \times (0, \infty)$,

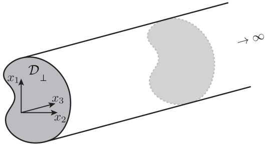

and find $p(x_1, x_2, x_3)$ such that

$$-\nabla^2 p - \kappa^2 p = 0 \text{ in } \mathcal{D}_\perp \times (0, \infty) \quad ,$$

subject to boundary conditions

$$p = q \text{ on } (x_1, x_2) \in \mathcal{D}_\perp, x_3 = 0,$$

$$\frac{\partial p}{\partial n} = 0 \text{ on } (x_1, x_2) \in \partial\mathcal{D}_\perp \times (0, \infty),$$

p (say) outgoing bounded wave as $x_3 \to \infty$.

Separation of Variables

Restrict attention to the transverse domain $\mathcal{D}_\perp$,

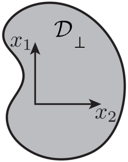

and find $(\Upsilon_i(x_1, x_2), \lambda_i)_{i=1,\ldots}$ solution of eigenproblem

$$-\nabla^2_{x_1,x_2}\Upsilon = \lambda\Upsilon \text{ in } \mathcal{D}_\perp \quad ,$$

$$\frac{\partial\Upsilon}{\partial n} = 0 \text{ on } \partial\mathcal{D}_\perp \quad ;$$

order (real) eigenvalues $\lambda_1 = 0 < \lambda_2 \leq \lambda_3 \leq \ldots$

Evanescence

Define n such that $\kappa \in [\sqrt{\lambda_n}, \sqrt{\lambda_{n+1}}[$: then

$$p(x;\kappa) = \sum_{j=1}^{n} \overbrace{c_j\,\Upsilon_j(x_1,x_2)\,e^{-\mathrm{i}\sqrt{\kappa^2-\lambda_j}\,x_3}}^{\text{propagating modes}} + \sum_{j=n+1}^{\infty} c_j\,\Upsilon_j(x_1,x_2)\,e^{\overbrace{-\sqrt{\lambda_j - k^2}}^{\text{real negative}}\,x_3}$$

for coefficients c_j chosen to realize $p(\cdot,\cdot,x_3=0)=q$.

Acoustics: $\kappa > 0 \Rightarrow n \geq 1$; one or more propagating modes.

Heat Conduction: $\kappa = 0 \Rightarrow n = 1$;

single "propagating" mode, $\Upsilon_1 \equiv$ Constant.

Equilibrium Elasticity: $\kappa = 0 \Rightarrow n = 6$; rigid-body modes.

Thermal Heatsink: Thermal Fins *in situ*

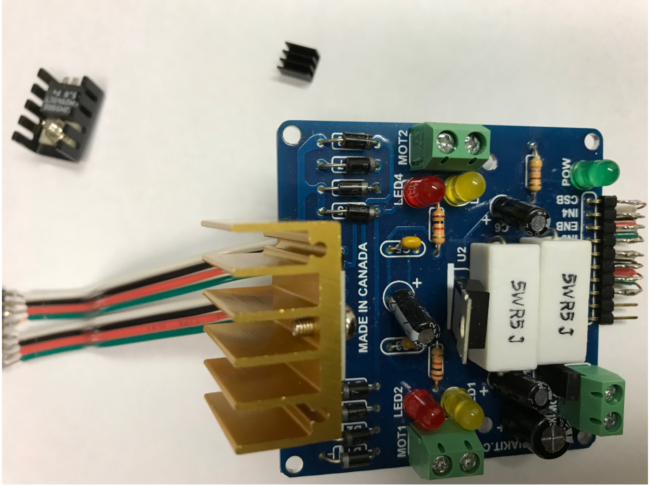

Library of Parametrized Archetype Components

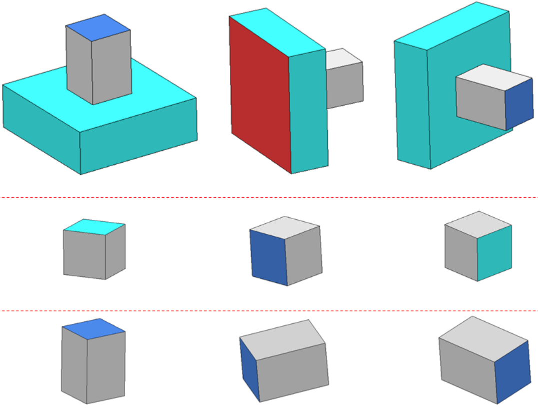

SPREADER

Parameters:
$H = [1.0, 2.0]$
$\eta_2 = [0.01, 0.5]$

FIN 1

Parameters:
$L_3 = [0.5, 2.0]$
$\eta_3 = [0.01, 0.5]$

FIN 2

Parameters:
$L_4 = [0.5, 2.0]$
$\eta_4 = [0.01, 0.5]$

Port | Zero flux | Heat flux | Robin surface | Temperature of zero

pPDE Model: System of Instantiated Components

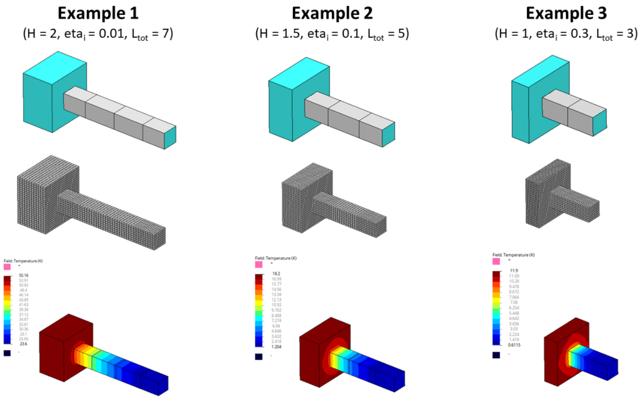

Encapsulated pPDE Model *Simple Heatsink*:

$$\mu_{\text{System}} \equiv (4\text{Bi}^{\text{fin}}, H, L_{\text{fin}}) \in \mathcal{P} \equiv [0.01, 0.5] \times [1, 2] \times [3, \infty[.$$

pPDE Model: System of Instantiated Components

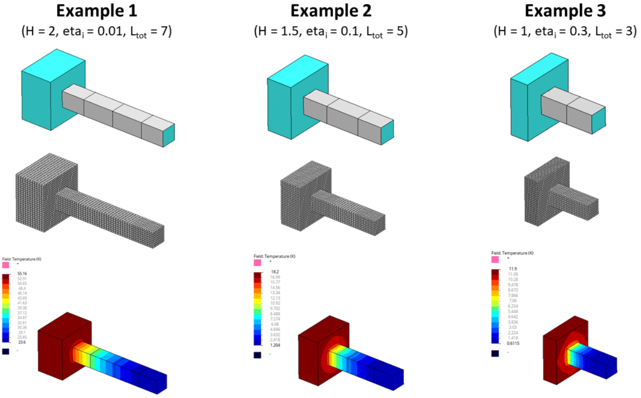

Encapsulated pPDE Model *Simple Heatsink*: BE estimation

$$\mu_{\text{System}} \equiv (4\text{Bi}^{\text{fin}}, H, L_{\text{fin}}) \in \mathcal{P} \equiv [0.01, 0.5] \times [1, 2] \times [3, \infty[.$$

pPDE Model: System of Instantiated Components

Example 1	Example 2	Example 3
($H = 2$, $eta_i = 0.01$, $L_{tot} = 7$)	($H = 1.5$, $eta_i = 0.1$, $L_{tot} = 5$)	($H = 1$, $eta_i = 0.3$, $L_{tot} = 3$)

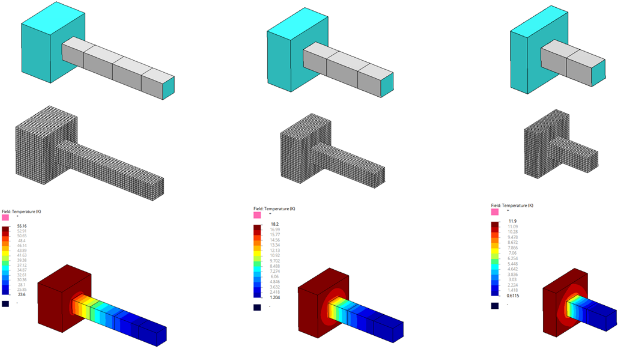

Encapsulated pPDE Model *Simple Heatsink*: BE incorporation

$$\mu_{\text{System}} \equiv (4\text{Bi}^{\text{fin}}, H, L_{\text{fin}}) \in \mathcal{P} \equiv [0.01, 0.5] \times [1, 2] \times [3, \infty[.$$

Offline Stage: Library [13, 30, 39, 34, 33]

Port Reduction: Evanescence [18, 10]

Train over all port-compatible archetype component *pairs*:

impose random Dirichlet conditions on unshared ports;

consider random parameter values within each component;

accumulate restriction of solution to shared port.

Perform POD on port restrictions for each port "color."

Bubble Reduction: Component Parametric Manifold

Train over all (single) archetype components:

for each port mode-cum-Dirichlet data:

consider random parameter values within component;

identify RB space for solution in interior of component.

Online Stage

Instantiation and Assembly: map μ_{System} to archetype component (local) parameters; connect (compatible) ports to form System.

Static Condensation: eliminate RB — *not* FE — bubble degrees of freedom within each instantiated component of System.

Direct Stiffness: construct Schur complement for System *reduced* port degrees of freedom — small and block-sparse.

Solution: apply sparse Gaussian elimination to Schur complement to obtain reduced port degrees of freedom.

Postprocessing: reconstruct RB bubble approximations in interiors of components from reduced port degrees of freedom.

Future Prospects: 2030

Headline:

Artificial Student Earns A+ in MIT Subject 2.51

Implications: in engineering education

How should we change *what* we teach,
and *how* we teach?

How should we change our assessment of (human) students?

and downstream, in professional engineering practice,

How can we enhance prediction procedures?

General theme: integrated methodology
for mathematical modeling and computation.

First (very brittle) steps: Artie [44].

Future Prospects: 2030

Headline:

and Accepts Employment as a ParaEngineer

Implications: in engineering education

How should we change *what* we teach,
and *how* we teach?

How should we change our assessment of (human) students?

and downstream, in professional engineering practice,

How can we enhance prediction procedures?

General theme: integrated methodology
for mathematical modeling and computation.

First (very brittle) steps: Artie [44].

References

[1] NH Afgan and M Da Graca Carvalho.
A confluence-based expert system for the detection of heat exchanger fouling.
Heat Transfer Engineering, 19(2):28–35, 1998.

[2] ASHRAE.
2017 ASHRAE Handbook - Fundamentals.
ASHRAE, Atlanta, GA, 2017.

[3] DG Bagby and RA Cormier.
A heat exchanger expert system.
AHSRAE Transactions, 95(2), 1989.

[4] J Ballani, P Huynh, D Knezevic, L Nguyen, and AT Patera.
PDE Apps for acoustic ducts: A parametrized component-to-system model-order-reduction approach.
In *ENUMATH, Voss, Norway*. Springer, 2018.

[5] J Ballani, P Huynh, D Knezevic, L Nguyen, and AT Patera.
PDE Apps for acoustic ducts: A parametrized component-to-system model-order-reduction approach.

In *Proceedings ENUMATH 2017, Voss, Norway*. Springer, 2018.

[6] P Binev, A Cohen, W Dahmen, G Petrova, and P Wojtaszczyk.
Convergence rates for greedy algorithms in reduced basis methods.
SIAM J Math Anal, 43(3):1457–1472, 2011.

[7] JP Birk.
The computer as student: an application of artifical intelligence.
J Chem Educ, 69(4):294–295, April 1992.

[8] DG Bobrow.
Natural language input for a computer problem solving system.
Technical Report Report MAC-TR-1, Project MAC, MIT, June 1964.

[9] D Braun, AH Mendez, F Matthes, and M Langen.
Evaluating natural language understanding services for conversational question answering systems.
In *Proceedings of the SIGDIAL 2017 Conference*, pages 174–185. Association for Computational Linguistics, 2017.

[10] A Buhr and K Smetana.

Randomized local model order reduction.
Preprint arXiv:1706.09179, 2018.

[11] SB Clemes, KGT Hollands, and AP Brunger.
Natural convection heat transfer from long horizontal isothermal cylinders.

Transactions of the ASME, 116:96–104, February 1994.

[12] WJ Cochran, D Hainley, and L Khartabil.
Knowledge based system for the design of heat exchangers.
In *SPIE Applications of Artificial Intelligence 1993: Knowledge-Based Systems in Aerospace and Industry*, volume 1963, 1993.

[13] RJ Craig and M Bampton.
Coupling of substructures for dynami analyses.
AIAA Journal, 3(4):678–685, 1968.

[14] NC Cuong, K Veroy, and AT Patera.
Certified real-time solution of parametrized partial differential equations.
In S Yip, editor, *Handbook of Materials Modeling*, pages 1529–1564. Springer, 2005.

[15] D Das, D Chen, AFT Martins, and NA Smith.
Frame-semantic parsing.
Computational Linguistics, 40(1), 2014.

[16] MO Deville, PF Fischer, and EM Mund.
High-Order Methods for Incompressible Fluid Flow.
Cambridge University Press, 2002.

[17] JL Eftan, AT Patera, and EM Ronquist.
An hp certified reduced basis method for parametrized elliptic partial differential equations.
SIAM J Sci Comput, 32:3170–3200, 2010.

[18] JL Eftang and AT Patera.
Port reduction in component-based static condensation for parametrized problems: Approximation and a posteriori error estimation.
IJNME, 96(5):269–302, 2013.

[19] W Elenbaas.
Heat dissipation of parallel plates by free convection.

Physica IX, 1:1–28, January 1942.

[20] HG Elrod.

Two simple theorems for establishing bounds on the total heat fow in steady-state heat-conduction problems with convective boundary conditions.

ASME J Heat Transfer, 96(1):65–70, 1974.

[21] L Fick, Y Maday, AT Patera, and T Taddei.

A stabilized POD model for turbulent flows over a range of Reynolds numbers: optimal parameter sampling and constrained projection.

J Computational Physics, 371:214–243, 2018.

[22] JR Finkel, T Grenager, and C Manning.

Incorporating non-local information into information extraction systems by Gibbs sampling.

In *Proceedings of the 43nd Annual Meeting of the Association for Computational Linguistics (ACL 2005)*, pages 363–370, 2005.

[23] MA Grepl and AT Patera.

A posteriori error for reduced-basis approximations of parametrized parabolic partial differential equations.

M2AN, 39(1):157–181, 2005.

[24] B Haasdonk and M Ohlberger.

Reduced basis method for finite volume approximation of parametrized linear evolution equations.

M2AN, 42(2):277–302, 2008.

[25] AV Hassani and KGT Hollands.

On natural convection heat transfer from three-dimensional bodies of arbitrary shape.

ASME Journal of Heat Transfer, 111:363–371, 1989.

[26] M Hess, A Alla, A Quaini, G Rozza, and Max G.

A localized reduced-order modeling approach for PDEs with bifurcating solutions.

Preprint arXiv:1807.08851, July 2018.

[27] JS Hesthaven, G Rozza, and B Stamm.

Certified reduced basis methods for parameterized partial differential equations.

Springer, 2016.

[28] J Hokanson.

Software `urlread2` for http requests and response processing in MATLAB, 2012.

[29] A Hormann.

Gaku: An artifical student.

Behavioral Science, 10:88–107, 1965.

[30] WC Hurty.

On the dynamics of structural systems using component modes.

AIAA Paper 64-487, 1964.

[31] DBP Huynh.

Software `GNLRequest`: Matlab client for Google Natural Language Processor, 2018.

[32] P Huynh, DJ Knezevic, and AT Patera.

A static condensation reduced basis element method: Approximation and a posteriori error estimation.
M2AN, 47(1):213–251, 2013.

[33] L Iapichino, A Quarteroni, and G Rozza.
Reduced basis method and domain decomposition for elliptic problems in networks and complex parametrized geometries.
Comput Math Appl, 71(1):408–430, 2016.

[34] L Iapichino, Q Quarteroni, and G Rozza.
A reduced basis nybrid method for the coupling of parametrized domains represented by fluidic networks.
CMAME, 221-222:63–82, 2012.

[35] JH Lienhard IV and JH Lienhard V.
A Heat Transfer Textbook.
Phlogiston Press, Fourth Edition, version 2.12 July 15, 2018, available at `http://ahtt.mit.edu` edition, 2018.

[36] N Kushman, Y Artzi, L Zettlemoyer, and R Barzilay.
Learning to automatically solve algebra word problems.

In *Proceedings 52nd Annual Meeting of the Association for Computational Linguistics*, 2014.

[37] HP Langtangen and A Logg.
Solving PDEs in Python - The FEniCS Tutorial Volume 1.
Springer, 2017.

[38] Google LLC.
Google Natural Language Processor.
https://cloud.google.com/natural-language/docs/, 2018.

[39] Y Maday and EM Ronquist.
The reduced basis element method: Application to a thermal fin problem.
SIAM Journal on Scientific Computing, 26(1):240–258, 2004.

[40] M Magen, BB Mikic, and AT Patera.
Bounds for conduction and forced convection heat transfer.
International Journal of Heat and Mass Transfer, 31(9):1747–1757, 1988.

[41] MathWorks.
MATLAB.

https://www.mathworks.com/.

[42] A Mukherjee and U Garain.
A review of methods for automatic understanding of natural language mathematical problems.
Artificial Intelligence Review, 29(2):93–122, 2008.

[43] Nek5000.
https://nek5000.mcs.anl.gov/.

[44] AT Patera.
Project Artie: An artificial student for disciplines informed by partial differential equations.
Technical report, arXiv (math), https://arxiv.org/abs/1809.06637, September 2018.

[45] P-O Persson.
Software `DistMesh` (MATLAB) for generation and manipulation of unstructured simplex meshes, 2004-2012.

[46] Q Qang, Z-H Wan, R Yan, and D-J Sun.

Multiple states and heat transfer in two-dimensional titled vonection with large aspect ratios.
Physical Review Fluids, 3(113503):1–28, 2018.

[47] A Quarteroni, A Manzoni, and F Negri.
Reduced basis methods for partial differential equations.
Springer, 2016.

[48] A Quarteroni and A Valli.
Numerical Approximation of Partial Differential Equations.
Springer, 2008.

[49] G Rozza and F Pichi.
Reduced basis methods for bifurcation analysis.
private communication.

[50] L Ridgway Scott.
Introduction to Automated Modeling with FEniCS.
Computational Modeling Initiative, 2018.

[51] F-Chart Software.

Engineering equation solver.

[52] Universal Technical Systems.

UTS Software, Heat Transfer 5.0, 2-18.

[53] B Szabó and I Babuška.

Introduction to Finite Element Analysis: Formulation, Verification and Validation.

Wiley, first edition, 2011.

[54] K Veroy and AT Patera.

Certified real-time solution of the parametrized steady incompressible Navier-Stokes equations: rigorous reduced-basis a posteriori error bounds.

International Journal for Numerical Methods in Fluids, 47(8-9):773–788, 2005.

[55] I Wang, J Akhtar, J Borggaard, and T Iliescu.

Propert orthogonal decomposition closure models for turbulent flows; a numerical comparison.

CMAME, 237:10–26, 2012.

[56] P Wang, R Kahawita, and DL Nguyen.
Transient laminar natural convection from horizontal cylinders.
International Journal of Heat and Mass Transfer, 34(6):1429–1442, 1991.

[57] EL Wilson.
The static condensation algorithm.
IJNME, 8(1):198–203, 1974.

[58] M Yano.
Software `fem2d` (MATLAB) for finite element solution of PDEs in two space dimensions, 2018.

[59] Masayuki Yano.
A space-time Petrov-Galerkin certified reduced basis method: Application to the Boussinesq equations.
SIAM Journal on Scientific Computing, 36(1):A232–A266, 2014.

[60] MM Yovanovich and P Teertstra.
Natural convection from horizontal finite length isothermal circular cylinders.

33rd Thermophysics Conference, AIAA Paper 99-3623, 1999.